nature portfolio

Peer Review File

Mitochondrial Rewiring with Small-Molecule Drug-Free Nanoassemblies Unleashes Anticancer Immunity

Mitochondrial Rewiring
with Small-Molecule
Drug-Free
Nanoassemblies
Unleashes Anticancer
Immunity

REVIEWER COMMENTS

Reviewer #1 (Remarks to the Author): with expertise in cancer immunology, immunogenic cell death

The present manuscript "Mitochondrial Rewiring with Small-Molecule Drug-Free Nanoassemblies Unleashes Anticancer Immunity" by Ren et al. describes the engineering and characterization of mitochondria-targeted dynamic supramolecular nanoassemblies (mtDSN) that consist of a fatty acid mixture assembled together with a mitochondria-targeting moiety, 3-(aminopropyl)triphenylphosphonium (TPP). The authors show that mtDSN2 has cytotoxic properties that induce cellular stress and ultimately cell death that shows traits of apoptosis and morphological and biochemical characteristics of paraptosis. Moreover, mtDSN2 treated cancer cells underwent premortem ER stress and exhibited hallmarks of immunogenic cell death such as calreticulin exposure, ATP release and HMGB1 exodus. Prophylactic vaccination with cancer cells dying in response to mtDSN2 immunized mice against rechallenge, decrease metastatic spread and positively altered the immune landscape. Intratumoral injection of mtDSN2 in tumor bearing mice showed efficacy on treated and syngeneic distant tumors along with increased CD8 T cell infiltration and this effect was antigen-specific. Moreover, mtDSN2 synergized with anti-PD-1 immune checkpoint inhibition (ICI) and rendered ICI insensitive tumor models sensitive to treatment.

The present manuscript is logically structured and extremely well written yet has some conceptual caveats.

Major:

As to show antigen (or cell type)-specificity the authors use 4T1 and B16F10 cells inoculated on contralateral flanks in Balb/c and follow growth of both tumors upon treatment of 4T1 tumors. B16F10 are derived from C57BL/6 an are spontaneously rejected in Balb/c. In the present manuscript though tumors thrive unrestricted which puts the general approach into question.

The effect of mtDSN2 needs to be shown on healthy tissue as well as on orthotopic tumors to allow evaluating the translational value of the presented findings.

Minor:

The generated PD-1 resistant cells should be further characterized to show the selected defect that allows evasion of immune destruction (that can be overcome by mtDSN2 treatment).

Immunoblots often only have one loading control despite multiple bands with distinct band patterns (even of phosphoneoepitope-specific and -unspecific antibodies). Of note all bands need to arise from one single blot (or need several loading controls). In any case full membrane scans should be annexed as sign of good scientific practice. In cases, where immunoblots are the sole evidence such as in Fig. 2 quantification is needed.

Mechanistic insights into cell death could be further addressed with cell death subroutine-specific knockouts.

Experiments depicted in Figure 6 are missing essential anti-PD1 monotreatment control groups.

Obvious triple combination of MPLA/mtDSN2/ICI should be tested.

The inhibitory effect of MPLA on mtDSN2 with regard to metastatic spread should be discussed.

Propidium iodide works exclusively in live cells as an exclusion dye. Fixing cells before staining as done by the authors is questionable.

Reviewer #2 (Remarks to the Author): with expertise in biomaterials, nanomedicine
In the manuscript "Mitochondrial Rewiring with Small-Molecule Drug-Free Nano-assemblies Unleashes Anticancer Immunity", Ren et al. reported the development of a class of small molecules that can recapitulate aqueous self-assembly behavior, dynamically rewire mitochondria, and invigorate tumor cell immunogenicity. The engineered mtDSN-2 showed

impressive anti-tumor activity in multiple preclinical mouse models, inflamed the immunologically silent TME and synergized with ICB therapy, leading to the prevention of metastatic recurrence and induction of protective memory. Overall, the story is very interesting. The manuscript follows a solid logical workflow for development and testing of a new immunotherapy formulation. However, a few issues need minor considerations and improvement before publication.

1. The authors demonstrated that mtDSN-2 impacted the mitochondrial ultrastructure using SEM analysis (Fig. 1g). It's very interesting that mitochondria were observed with huge cavities and warped configuration after directly adding mtDSN-2 on isolated mitochondria. However, the authors should exclude the possibility that the damage of mitochondria is caused by the preservation of mitochondria at 4°C for 30 min. A control group should be included for comparison.

2. mtDSN-2 induced significant mitochondrial damage and ER swelling in Hela/R cells as evidenced by TEM observation in Figure 1f. Whether this phenomenon is extensively existed in other cancer cells treated with mtDSN-2? It's recommended to verify in other cancer cells such as 4T1 cells.

3. More details about the experiments should be given. (1) how to determine the citrate synthase activity? (2) how to determine the ER mass enlargement?

4. Line 90, the authors write: "By sharp contrast, the TPP moiety or fatty acids alone as well as the simple mixture of both molecules were not cytotoxic and did not affect cell viability (Supplementary Table 2)." According to the results from Supplementary Table 2, the simple mixture of TPP moiety and fatty acids actually caused certain cytotoxicity with IC50 of 50-80 μM in A2780 cells. Hence, it's not appropriate to conclude that these molecules were not cytotoxic and did not affect cell viability.

5. Line 244, the authors should specify the mass enlargement and swelling of ER rather than mitochondria to avoid ambiguity.

6. The authors should offer the exact sample size (n) or the statement of measurement repetition for each experiment, especially studies that were qualitatively analyzed.

Reviewer #3 (Remarks to the Author): with expertise in biomaterials, nanomedicine
In this study, the authors synthesized self-assembling nanodrugs by covalently linking TPP

with various fatty acids. Excitingly, these drug-free nanoassemblies demonstrated cytotoxicity. The authors selected the nanodrug with the most potent cytotoxicity for mechanistic investigation and found that it could target and remodel mitochondria, inducing cell death in an apoptosis and paraptosis-dependent manner. Additionally, this nanoformulation exhibited the potential as a specific tumor preventive vaccine, displayed excellent antitumor effects, and enhanced the efficacy of ICB therapy, successfully converting the "cold" tumor microenvironment into a "hot" one. This study provides a powerful approach to overcome immune suppression in solid tumors. Overall, the strategy is innovative, and these new drug-free compounds are potentially useful for oncology drug development. The manuscript is well-written, and the experimental data are abundant and complete. I recommend accepting this article with a slight modification:

1. It is recommended to evaluate the stability of the selected formulations such as FBS stability, or the long-term stability of these compounds when stored, to ensure that the formulations remain stable and intact following cytotoxic drug administration.

2. In Figure 1c, it is shown that the Cy5.5-labeled nanoassemblies can co-localize with mitochondrial dyes, indicating that mtDSN-2 binds to mitochondria in the form of nanoparticles rather than as free molecules. Please explain why TPP-LA conjugate 2 can still achieve mitochondrial targeting after forming nanoparticles.

3. By what pathway do the nanoparticles enter the cells? Do the mtDSN-2 undergo lysosome escape? Please investigate the co-localization of mtDSN-2 with lysosomes and describe the intracellular transport process of mtDSN-2.

4. Since the mitochondrial damage caused by the formulation is not selective, it can be also expected to impart the cytotoxicity onto immune cells. Thus, the authors should provide reasonable explanation why mtDSN-2 can inflame the tumors to prime the antitumor immunity.

5. Please provide a detailed description of the experimental protocol for quantifying drug concentrations after formulation dialysis.

Reviewer #4 (Remarks to the Author): with expertise in cancer, cell death

The manuscript "Mitochondrial Rewiring with Small-Molecule Drug-Free Nanoassemblies Unleashes Anticancer Immunity" offers a promising nondrug immune enhancer and

describes its mechanisms of mitochondrial/ER-associated immunogenic cell death to overcome immunosuppression in solid tumors. Showing various in vivo evidence, the authors suggest that this new mitochondria-targeting and rewiring platform as a promising new strategy to achieve non-cytotoxic cancer therapy. I think that authors' suggestion is supported by appropriate evidence, and believe if this research further develops, it could be a promising strategy to overcome the current issues of resistance in immunotherapy. Overall, this manuscript deals with a relevant topic likely to be of considerable interest to the broader scientific cancer community, but there are some issues needed to describe more.

1. Based on my understanding, the cell death mechanisms induced by mtDSN-2 are paraptosis and apoptosis, with TPP acting as a carrier that transports LA to the mitochondria. Therefore, it seems that cell death is caused by the excessive accumulation of LA within the mitochondria. In this case, would the phenomenon observed with mtDSN-2 be the same result when treating cells with a high concentration (IC50) of LA only?

2. To verify the cytotoxicity of mtDSNs, various cell lines were used, including cisplatin-resistant cancer cells. It would be beneficial to explain the reason why you used especially cisplatin-resistant cancer cells as well.

3. To conclusively show there is a cytosolic release of cytochrome c in Figure 2k, the mitochondria should also be displayed.

4. Beside to HRI-dependent eIF2a phosphorylation (line 253), there is PERK activation by mtDSN-2 (Fig. 3o). Furthermore, ER swelling is evident in Figure 3n. Based on that I am curious whether there is a direct impact or accumulation of mtDSN-2 on the ER. Additionally, is there any swelling of the ER observed in TEM consistent with fluorescent image in Figure 3n?

5. In Figure 3e, measuring the extracellular level of HMGB1 rather than its cytosolic level would provide more accurate evidence of immunogenic cell death (ICD).

6. The evidence for paraptosis appears insufficient, as it relies solely on ER/mitochondria swelling and death blocked by CHX. Since CHX is known to inhibit not only paraptosis but also ER stress-induced cell death, it appears crucial to present changes in other markers of paraptosis.

7. Have you conducted tests on the impact of mtDSN-2 on normal cells? Does the

accumulation of mtDSN-2 on the mitochondria of normal cells or immune cells occur? What is the cancer-specific targeting mechanism of mtDSN-2?

8. A more detailed discussion is needed on the underlying mechanism (or possible explanation) by which mitochondrial stress induction by mtDNS-2 lead to ICD.

9. Please write the concentrations of each inhibitor presented in Figure 2.

10. The composition of each mtDSN conjugate 1 to 5 should be specified in the text. For example, specify that conjugate 2 is TPP-LA in lines 92-93.

RESPONSE TO REVIEWERS – NCOMMS-24-15112

Reviewer #1 (Remarks to the Author)

The present manuscript "Mitochondrial Rewiring with Small-Molecule Drug-Free Nanoassemblies Unleashes Anticancer Immunity" by Ren et al. describes the engineering and characterization of mitochondria-targeted dynamic supramolecular nanoassemblies (mtDSN) that consist of a fatty acid mixture assembled together with a mitochondria-targeting moiety, 3-(aminopropyl)triphenylphosphonium (TPP). The authors show that mtDSN2 has cytotoxic properties that induce cellular stress and ultimately cell death that shows traits of apoptosis and morphological and biochemical characteristics of paraptosis. Moreover, mtDSN2 treated cancer cells underwent premortem ER stress and exhibited hallmarks of immunogenic cell death such as calreticulin exposure, ATP release and HMGB1 exodus. Prophylactic vaccination with cancer cells dying in response to mtDSN2 immunized mice against rechallenge, decrease metastatic spread and positively altered the immune landscape. Intratumoral injection of mtDSN2 in tumor bearing mice showed efficacy on treated and syngeneic distant tumors along with increased CD8 T cell infiltration and this effect was antigen-specific. Moreover, mtDSN2 synergized with anti-PD-1 immune checkpoint inhibition (ICI) and rendered ICI insensitive tumor models sensitive to treatment. The present manuscript is logically structured and extremely well written yet has some conceptual caveats.

Response:

We thank the reviewer very much for his/her positive comments and useful suggestions, which helped us to improve the manuscript.

Major:

As to show antigen (or cell type)-specificity the authors use 4T1 and B16F10 cells inoculated on contralateral flanks in Balb/c and follow growth of both tumors upon treatment of 4T1 tumors. B16F10 derived from C57BL/6 are spontaneously rejected in Balb/c. In the present manuscript though tumors thrive unrestricted which puts the general approach into question.

Response:

Many thanks for raising this very important point. According to the Reviewer's suggestion, we additionally established a bilateral tumor model by inoculating Balb/c-

derived 4T1 and CT26 cells on the right and left flanks of Balb/c mice, respectively, to examine the specificity of antitumor T-cell responses. These new results are shown in revised Fig. 5g-i. Two intratumoral injections of mtDSN-2 to the right 4T1 tumor significantly inhibited the growth of the primary 4T1 tumor. In sharp contrast, contralateral CT26 tumor burden was observed without abscopal effect, indicating the tumor-specific immunity elicited by mtDSN-2. We have supplemented the relevant data in the new Fig. 5g-i, and the comments are also incorporated into the revised manuscript, page 7, as follows:

To probe the specificity of the T-cell responses, we used unrelated CT26 colorectal cancer cells instead of 4T1 breast cancer cells as the contralateral tumor (Fig. 5g). In that case, mtDSN-2 suppressed the local tumor (Fig. 5h) but exerted no abscopal tumor control, as contralateral CT26 tumors displayed rapid growth kinetics comparable to those of saline-treated mice (Fig. 5i).
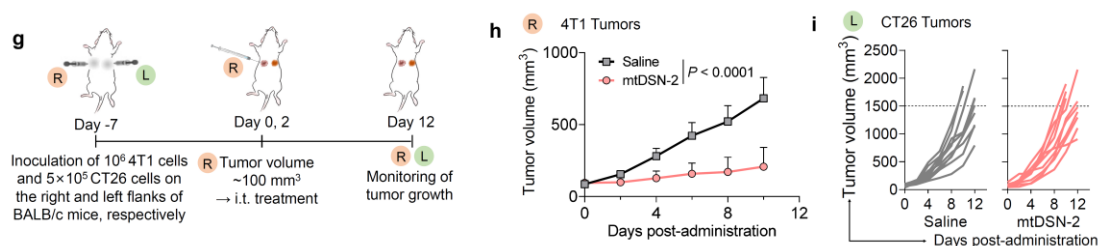
Figure 5. g, Schedule of bilateral heterologous tumor inoculation in BALB/c mice and treatment. **h** and **i**, Growth profiles of primary 4T1 tumors (**h**) and distant CT26 tumors (**i**) (n = 10 mice/group).
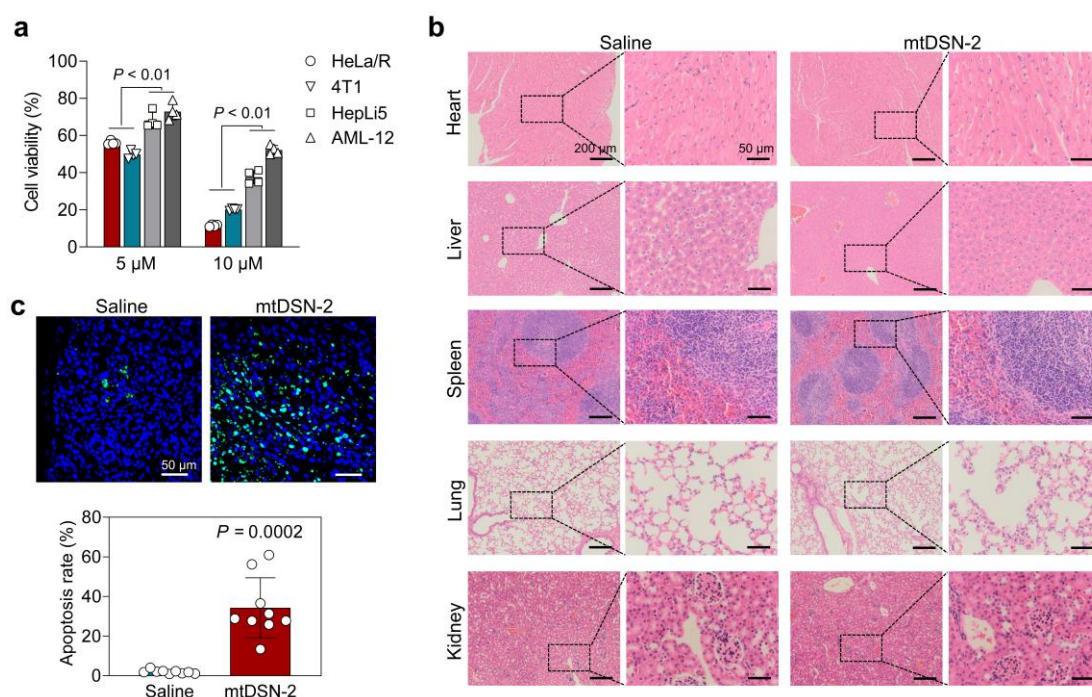
The effect of mtDSN2 needs to be shown on healthy tissue as well as on orthotopic tumors to allow evaluating the translational value of the presented findings.

Response:

Per your suggestion, we used an orthotopic 4T1 tumor model to evaluate the potential effect of mtDSN-2 on healthy tissue as well as on orthotopic tumors. After intratumoral injections of mtDSN-2, the tumors and major organs were collected and subjected to histological analysis. As shown in Supplementary Fig. 30, mtDSN-2 induced extensive apoptosis of tumor cells indicated by TUNEL staining. In H&E staining, the major organs (i.e., heart, liver, spleen, lung and kidney) of mice did not present any obvious damages after mtDSN-2 treatment, comparable to those of mice receiving saline. In addition, according to another Reviewer's comment, we have

evaluated the cytotoxicity of mtDSN-2 in normal cell lines such as HepLi5 and AML12 hepatocytes. These new results are presented in Supplementary Fig. 30, and the relevant comments are also added in the revised manuscript, page 11, as follows:

Indeed, mtDSN-2 was less cytotoxic on hepatocytes than on cancer cells observed in in vitro assays (Supplementary Fig. 30a). Intratumoral administration of mtDSN-2 did not impart any side effects on major healthy tissues (Supplementary Fig. 30b) while inducing extensive apoptotic cell death in tumors (Supplementary Fig. 30c), suggesting its favorable safety profile for the preclinical use.

Figure S30. a, Cytotoxicity of mtDSN-2 (5 μM or 10 μM for 48 h) in cancer cells (HeLa/R) and hepatocytes (AML12 and HepLi5) determined using MTT assay (n = 4). **b**, H&E staining of the major organs (n = 3 mice/group) after drug administration. **c**, Immunohistochemical analysis of the tumor apoptosis by TUNEL staining (n = 3 mice/group). The data are presented as the mean ± s.d. Statistical analysis by one-way ANOVA with Turkey's multiple comparisons test, Brown-Forsythe and Welch ANOVA with Dunnett's T3 multiple comparisons test (**a**) and Student's t test (**c**).

Minor:

The generated PD-1 resistant cells should be further characterized to show the selected defect that allows evasion of immune destruction (that can be overcome by mtDSN2 treatment).

Response:

Patients with initial response to immune checkpoint blockade treatment eventually develop therapeutic resistance. To test whether mtDSN-2 can potentiate anti-PD-1 therapy, we established a clinically relevant anti-PD-1-resistant MC38 tumor model through the repeated administration of anti-PD-1 antibodies followed by serial implantation (Fig. 7a). After three-cycle resistance induction, PD-1 blockade exhibited negligible tumor-suppressive activity in serially implanted S3 tumors compared with that in S0 parental tumors, suggesting the acquired resistance of S3 MC38 tumors to anti-PD-1 therapy (Fig. 7b). Moreover, according to the Reviewer's comment, we profiled the tumor microenvironment (TME) in S3 tumors by immunostaining. We observed notable CTL exclusion (Fig. 7c and d) and antitumorigenic M1 to protumorigenic M2 macrophage polarization in S3 tumors (Supplementary Fig. 24), which confirmed immune desertification of the TME and acquired resistance established in this model. Notably, mtDSN-2 administration reshaped the TME of S3 tumors by inducing the M2-to-M1 repolarization of macrophages (Supplementary Fig. 24) and promoting remarkable infiltration of tumor-killing CTLs (Fig. 7i and j), supporting the immunostimulatory effects of the mtDSN platform. More importantly, the immune landscape changes of the tumor tissues following mtDSN-2 treatment was further analyzed by the high-dimensional interrogation of tumors with scRNA-seq (Fig. 8). The new data and relevant description are supplemented in the revised manuscript, page 9, and Supplementary Fig. 24.

mtDSN inflames the tumor microenvironment to enhance the ICB response

Despite the compelling clinical benefits of PD-1 blockade in various types of malignant cancer, patients eventually develop acquired resistance to this therapy after an initial response. To address this, we established an anti-PD-1-resistant MC38 tumor model through the repeated administration of anti-PD-1 antibodies followed by serial implantation (Fig. 7a). Although PD-1 blockade exhibited significant tumor-suppressive activity in S0 (parental) tumors, serially implanted S3 tumors (termed MC38/R) were refractory to anti-PD-1 therapy (Fig. 7b). Immunostaining also revealed notable CTL exclusion (Fig. 7c and d) and macrophage polarization from antitumorigenic M1 to protumorigenic M2 in MC38/R tumors (Supplementary Fig. 24) compared with that in parental tumors, confirming the immune desertification of the TME and the acquired resistance established in this model. Subsequently, we assessed the effects of mtDSN-2 on proinflammatory remodeling of the TME and its synergism with anti-PD-1 therapy to increase immune response in this clinically relevant tumor model. The mtDSN-2

therapy caused significant MC38/R tumor regression and extended mouse survival (Fig. 7e–h). Notably, M2-to-M1 repolarization of macrophages (Supplementary Fig. 24), abundance of intratumoral dendritic cells, and remarkable increase in tumor-infiltrating CTLs (Fig. 7i and j) supported the hypothesis that mtDSN-2 exerts immunomodulatory effects on tumors. More significantly, the combined mtDSN and anti-PD-1 regimen displayed a synergistic effect, with complete antitumor responses in six of nine mice and a striking increase in mice survival rate over 60 days (Fig. 7e–h).
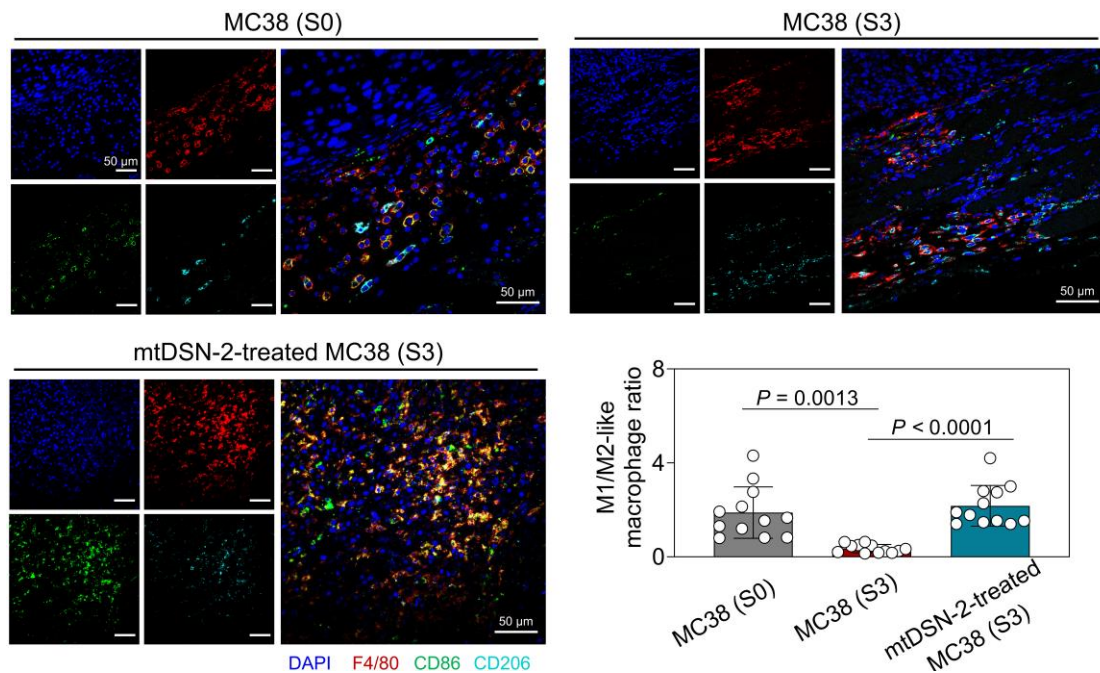
Figure S24. Immunofluorescence observation and quantitative analysis of tumor-associated macrophages (TAMs) in S0, S3 and mtDSN-2 treated S3 tumors. M1-like macrophage, stained by F4/80 and CD86; M2-like macrophage, stained by F4/80 and CD206. The representative images and quantification of M1/M2-like macrophage ratio are shown from three independent samples. The data are presented as the mean ± s.d. Statistical analysis by Brown-Forsythe and Welch ANOVA with Dunnett's T3 multiple comparisons test.

Immunoblots often only have one loading control despite multiple bands with distinct band patterns (even of phosphoneoepitope-specific and -unspecific antibodies). Of note all bands need to arise from one single blot (or need several loading controls). In any case full membrane scans should be annexed as sign of good scientific practice. In cases, where immunoblots are the sole evidence such as in Fig. 2 quantification is needed.
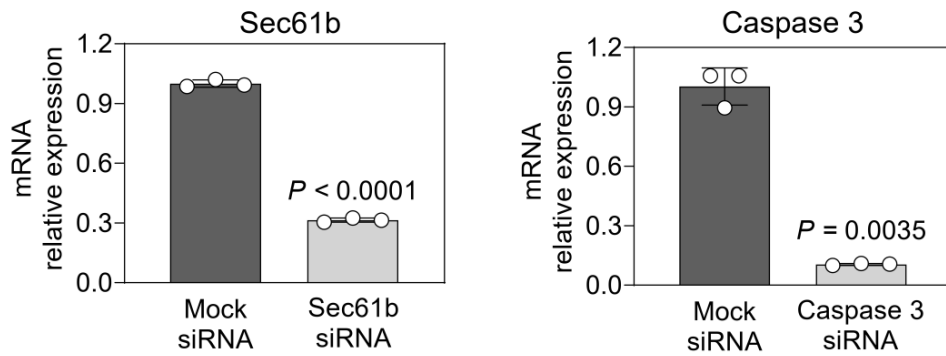
Response:

We have checked our original immunoblot data to make sure that every band has its own loading control from one single blot. Moreover, the band intensities for all immunoblots were quantitatively analyzed relative to their own loading control. The data repetition was stated in the figure legends. The original immunoblot data with protein markers were also updated as Source Data.

Mechanistic insights into cell death could be further addressed with cell death subroutine-specific knockouts.
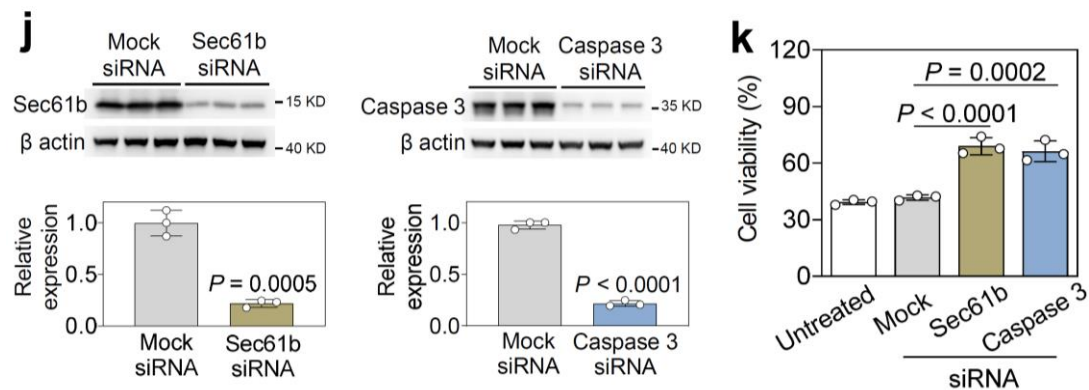
Response:

Many thanks for this important comment. Our previous results indicate that pharmacological inhibition of apoptosis and paraptosis, rather than necroptosis, ferroptosis and pyroptosis, enables to rescue mtDSN-2-induced cell death. According to the Reviewer's comment, we sought to further identify the programs driving cell death using apoptosis or paraptosis-specific-knockdown tumor cells. Caspase 3 and Sec61b have emerged as key contributors in mediating apoptosis and paraptosis, respectively [1-3]. We therefore constructed caspase 3 or Sec61b-knockdown 4T1 cells using siRNA-mediated silencing, as indicated by the qPCR and western blot results (Supplementary Fig. 13 and Fig. 2j). Importantly, silencing of caspase 3 or Sec61b inhibited mtDSN-2-triggered cell death (Fig. 2k), supporting a mitochondrial paraptosis/apoptosis mechanism. The relevant results are presented in Fig. 2j, k and Supplementary Fig. 13, and the data are discussed in the revised manuscript, page 5, as follows:

Sec61b and caspase 3 are crucial in mediating paraptosis and apoptosis, respectively. Intriguingly, we found that silencing Sec61b and caspase 3 inhibited the mtDSN-2-induced cell death (Fig. 2j, k and Supplementary Fig. 13). This finding further supports the proposed mechanism by which mtDSN-2 induces lethal mitochondrial paraptosis/apoptosis.

Figure S13. a, Relative mRNA expression in 4T1 cells transfected with mock (untargeted), Sec61b or caspase 3 siRNA. The data are presented as the mean ± s.d. The results were shown from three biologically independent repeats. Statistical analysis by Student's t test.

Figure 2. mtDSN induces cell death in an apoptosis and paraptosis-dependent manner. j, Immunoblotting analysis and quantification of 4T1 cells transfected with mock (untargeted), Sec61b or caspase 3 siRNA. **k**, Cell viability of 4T1 cells transfected with mock, Sec61b or caspase 3 siRNA followed by exposure to mtDSN-2.

Experiments depicted in Figure 6 are missing essential anti-PD1 monotreatment control groups. Obvious triple combination of MPLA/mtDSN2/ICI should be tested.

Response:

   The results in Fig.4 indicated that mtDSN-2-pulsed tumor cells are immunogenic and can be used as prophylactic vaccine. Moreover, the mtDSN scaffold could initiate ICD-induced tumor-specific T-cell activation, thereby boosting effective antitumor immunity against established local 4T1 tumors and yielding abscopal effect (Fig.5). Inspired by these results, we then sought to investigate the potential of mtDSN-2 in

combination with other treatments such as toll-like receptor agonists or immune checkpoint blockade therapy for their synergy. In the 4T1 tumor model, intratumoral combination of mtDSN-2 with MPLA or anti-PD-1 antibody improved the tumor-suppressive effect (Fig. 6a) and mouse survival extension (Fig. 6b) of mtDSN-2 monotherapy, and led to abundant infiltration of CD8^{+} T cells in tumors (Fig. 6c). However, the combination with MPLA was less efficient than that with anti-PD-1 for tumor metastasis inhibition. Hence, we further explored the synergy of mtDSN-2 and anti-PD-1 in MC38, anti-PD-1-resistant MC38, and CT26 tumor models (Fig. 6f-o and Fig.7), where anti-PD1 monotherapy was included for comparison.

According to your suggestion, we additionally performed the efficacy testing of anti-PD1 monotherapy and triple combination (i.e., MPLA, mtDSN2, and anti-PD1) in the orthotopic 4T1 tumor model. As shown in the below Figure R1, monotherapies using mtDSN-2 or anti-PD1 antibody suppressed the tumor growth compared with saline and MPLA treatment. Significantly, triple combination (COMB) exhibited durable tumor regression with the best activity and three out of eight mice cured.
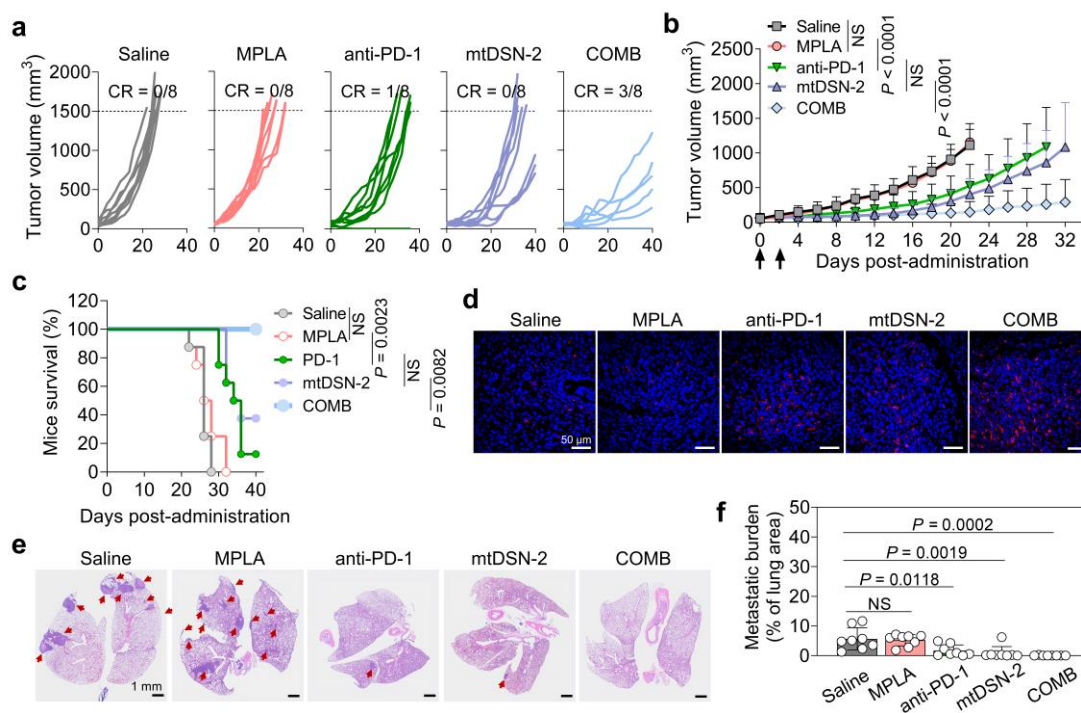
Figure R1. a and **b**, Individual (**a**) and average (**b**) orthotopic 4T1 tumor growth profiles after different treatments (n = 8 mice/group). COMB, mice treated with the combination of MPLA, anti-PD-1 and mtDSN-2. **c**, Kaplan–Meier survival of 4T1 tumor-bearing BALB/c mice. **d**, Immunofluorescence staining of the tumor sections showed CD8^{+} T-cell infiltration. Triplicates were performed independently with similar results. **e**, H&E staining images of lung tissue sections. Red arrows indicate metastatic foci. The

representative images are shown from eight independent samples. **f**, Quantification of the metastatic foci in lung tissues (n = 8 mice/group). Mice were sacrificed and lungs were excised for analysis when tumor volume exceeded 1500 mm^3 or at the endpoint of the experiment. The data are presented as the mean ± s.d. NS: not significant. Statistical analysis by two-way ANOVA with Turkey's multiple comparisons test (**b**), log-rank test (**c**), and one-way ANOVA with Turkey's multiple comparisons test (**f**).

The inhibitory effect of MPLA on mtDSN2 with regard to metastatic spread should be discussed.

Response:

Thanks for this important comment. We have added the relevant discussion in the revised manuscript, page 8, as follows:

Previous studies suggested a link between TLR4 activation and augmented metastatic phenotypes of cancer cells. TLR4 activation also was associated with local and systemic inflammation, creating the TME (e.g., reconstructed tumor-associated lymphatic and blood vessels) that favors tumor recurrence and metastasis. Hence, these effects of TLR4 agonist MPLA may account for the impaired metastatic inhibition of mtDSN-2.

Propidium iodide works exclusively in live cells as an exclusion dye. Fixing cells before staining as done by the authors is questionable.

Response:

Thanks for this comment. Calreticulin (CRT) is normally secluded in the ER lumen and relocates to the outer surface of the plasma membrane when cells undergoing ER stress during ICD [4]. For flow cytometry analysis of cell surface exposure of CRT in this study, tumor cells were treated with different agents, and then were carefully harvested using cell scrapers, washed twice with cold PBS, fixed in 0.25% paraformaldehyde for 5 min, and blocked with 3% fetal bovine serum for 15 min. Then, cells were incubated with anti-CRT antibody or isotype control antibody at 4°C for 30 min. After washed with PBS for three times, cells reacted with donkey anti-rabbit IgG Alexa FluorTM 488 at 4°C for 30 min. The cells were then stained with PI before flow cytometry examination. The cells were gated on PI-negative cells.

Fixation with paraformaldehyde (PFA) is the most widely used method for

downstream flow cytometry analyses. Many PFA-based protocols exist citing the PFA concentrations ranging from 1 to 4% for fixing about 15 min [5], after which cells are permeable to propidium iodide and might be stained by antibodies against intracellular proteins to some extent. In this study, we fixed cell samples in 0.25% PFA for 5 min on ice before incubation with anti-CRT antibody, according to the reported protocol for flow cytometric analysis of cell surface expose of CRT [6]. The PFA concentration and incubation time (0.25% for 5 min) are much lower than that in universal standard protocol of cell fixation (4% for 15 min), and didn't lead to the cell permeation of PI and antibodies, as indicated by the majority of PI-negative cells (Fig. R2) and significantly lower CRT signal in drug untreated group (Fig. 3b and Supplementary Fig. 14) after 0.25% paraformaldehyde fixation for 5 min.

In addition, PI-negative cells are naturally impermeable to CRT antibodies when staining. Hence, we stained the cells with PI after antibodies incubation and analyzed the CRT signal of tumor cells gated on PI-negative cells to avoid false-positive cells (CRT signal from endoplasmic reticulum rather than cell membrane).
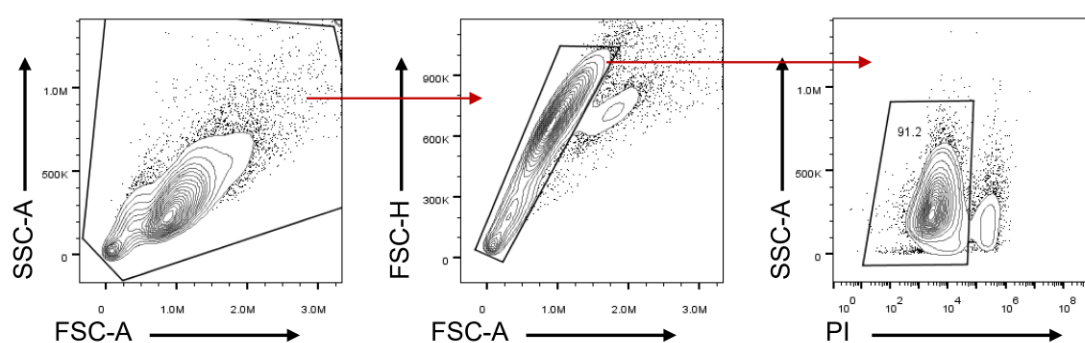
Figure R2. Gating scheme for flow cytometric analysis of cell surface exposure of CRT.

Reviewer #2 (Remarks to the Author)

In the manuscript "Mitochondrial Rewiring with Small-Molecule Drug-Free Nano-assemblies Unleashes Anticancer Immunity", Ren et al. reported the development of a class of small molecules that can recapitulate aqueous self-assembly behavior, dynamically rewire mitochondria, and invigorate tumor cell immunogenicity. The engineered mtDSN-2 showed impressive anti-tumor activity in multiple preclinical mouse models, inflamed the immunologically silent TME and synergized with ICB therapy, leading to the prevention of metastatic recurrence and induction of protective

memory. Overall, the story is very interesting. The manuscript follows a solid logical workflow for development and testing of a new immunotherapy formulation. However, a few issues need minor considerations and improvement before publication.

Response:

We thank the Reviewer very much for providing positive feedback on our work and raising many useful comments and suggestions, which helped us to improve the manuscript.

1. The authors demonstrated that mtDSN-2 impacted the mitochondrial ultrastructure using SEM analysis (Fig. 1g). It's very interesting that mitochondria were observed with huge cavities and warped configuration after directly adding mtDSN-2 on isolated mitochondria. However, the authors should exclude the possibility that the damage of mitochondria is caused by the preservation of mitochondria at 4°C for 30 min. A control group should be included for comparison.

Response:

Thank you for highlighting this issue. In all experimental groups, mitochondria were isolated from tumor cells and incubated at 4°C for 30 min with or without 0.5 μM mtDSN-2 before being fixed with 2.5% glutaraldehyde at room temperature for 2 h and overnight at 4°C. This protocol ensures that mitochondrial damage is not due to preservation at 4°C for 30 min, as evidenced by the thread-like mitochondria with intact membrane in untreated cells (**Fig. 1g**). We have elaborated on the experimental methods in the manuscript to clarify this point. The relevant comments are supplemented in the revised manuscript, page 27, as follows:

For SEM characterization, mitochondria isolated from tumor cells were incubated at 4°C for 30 min with or without 0.5 μM mtDSN-2, then fixed with 2.5% glutaraldehyde at room temperature for 2 h, followed by overnight at 4°C. Subsequently, the cells were washed three times with PBS, fixed with 1% osmium tetroxide, dehydrated through a graded series of ethanol concentrations (30, 50, 70, 80, 90, and 95% for 15 min each time and 100% for 20 min twice). After vacuum drying, the samples were coated with gold/palladium and analyzed by SEM using a Nova Nano 450 (Thermo).

2. mtDSN-2 induced significant mitochondrial damage and ER swelling in Hela/R cells as evidenced by TEM observation in Figure 1f. Whether this phenomenon is extensively existed in other cancer cells treated with mtDSN-2? It's recommended to

verify in other cancer cells such as 4T1 cells.

Response:

Following the Reviewer's suggestion, we conducted additional experiments using 4T1 cells. Consistent with our previous observations in HeLa/R cells using TEM, mtDSN-2 treatment also induced significant mitochondrial damage and ER swelling in 4T1 cells. These findings are presented in Supplementary Fig. 10. To reflect this update, we have amended the text on page 4 of the revised manuscript as follows:

Mitochondrial damages similar to that observed in HeLa/R cells were also evident in mtDSN-2-treated 4T1 cells (Supplementary Fig. 10).
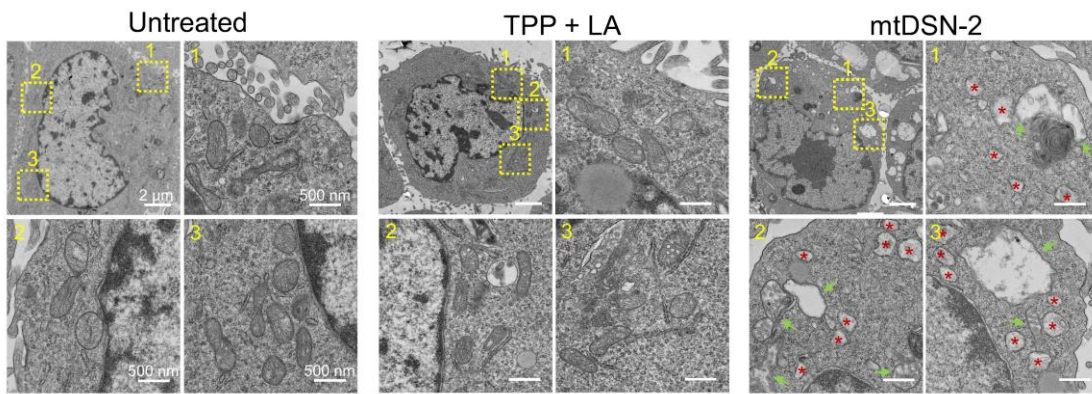
Figure S10. TEM images of mitochondrial ultrastructure in 4T1 cancer cells following various treatments. Green arrows point to damaged mitochondria, while red asterisks mark areas of swelling endoplasmic reticulum. These images represent findings from three biologically independent experiments.

3. More details about the experiments should be given. (1) how to determine the citrate synthase activity? (2) how to determine the ER mass enlargement?

Response:

Thank you for your thorough review. We have incorporated the details of these experiments into the revised supplementary information, pages 5-6, as follows:

Citrate synthase activity

Cells were treated with various agents at a concentration of 5 μM for 48 h. Subsequently, mitochondria were isolated from the cells to measure citrate synthase activity using a citrate synthase activity assay kit (Solarbio, China) following the manufacturer's protocol.

ER mass enlargement

Cells were treated with various agents at a concentration of 5 μM for 36 h. Then, cells were stained with 500 nM of ER tracker green (Beyotime, China) at 37°C for 30 min, followed by flow cytometry analysis and CLSM observation.

4. Line 90, the authors write: "By sharp contrast, the TPP moiety or fatty acids alone as well as the simple mixture of both molecules were not cytotoxic and did not affect cell viability (Supplementary Table 2)." According to the results from Supplementary Table 2, the simple mixture of TPP moiety and fatty acids actually caused certain cytotoxicity with IC50 of 50-80 μM in A2780 cells. Hence, it's not appropriate to conclude that these molecules were not cytotoxic and did not affect cell viability.

Response:

According to the Reviewer's suggestion, we have amended the wording in the revised manuscript, page 3, as follows:

In stark contrast, cells treated with either the TPP moiety or fatty acids alone, or with a simple mixture of both, exhibited low cytotoxicity and demonstrated negligible effects on cell viability (Supplementary Table 2).

5. Line 244, the authors should specify the mass enlargement and swelling of ER rather than mitochondria to avoid ambiguity.

Response:

According to the Reviewer's comment, we have specified the mass enlargement and swelling of ER to avoid ambiguity. The relevant comments are added to the revised manuscript, page 6, as follows:

Flow cytometry analysis (Fig. 3l and m) and CLSM observation (Fig. 3n) revealed ER mass enlargement and swelling in cells exposed to mtDSN-2, indicating notable ER perturbation.

6. The authors should offer the exact sample size (n) or the statement of measurement repetition for each experiment, especially studies that were qualitatively analyzed.

Response:

We have given the exact sample size (n) and the statement of measurement repetition in the figure legends.

In this study, the authors synthesized self-assembling nanodrugs by covalently linking TPP with various fatty acids. Excitingly, these drug-free nanoassemblies demonstrated cytotoxicity. The authors selected the nanodrug with the most potent cytotoxicity for mechanistic investigation and found that it could target and remodel mitochondria, inducing cell death in an apoptosis and paraptosis-dependent manner. Additionally, this nanoformulation exhibited the potential as a specific tumor preventive vaccine, displayed excellent antitumor effects, and enhanced the efficacy of ICB therapy, successfully converting the "cold" tumor microenvironment into a "hot" one. This study provides a powerful approach to overcome immune suppression in solid tumors. Overall, the strategy is innovative, and these new drug-free compounds are potentially useful for oncology drug development. The manuscript is well-written, and the experimental data are abundant and complete. I recommend accepting this article with a slight modification:

Response:

Many thanks for your critical reading and positive comments on our manuscript. Your valuable suggestions have greatly contributed to the improvement of the quality of this work.

1. It is recommended to evaluate the stability of the selected formulations such as FBS stability, or the long-term stability of these compounds when stored, to ensure that the formulations remain stable and intact following cytotoxic drug administration.

Response:

Thanks for raising these points. We first tested the storage stability of the conjugates **1-5** for 60 days using HPLC analysis. As indicated in Supplementary Fig. 6, all compounds were stable without changes of retention times in the HPLC spectra. In addition, the selected nanoformulations (e.g., mtDSN-2) remained thermodynamically stable for several days, and there was no visible precipitation in

deionized water, phosphate-buffered saline (PBS), and PBS with 10% fetal bovine serum (Supplementary Fig. 8). We have added the results in Supplementary Fig. 6 and 8, and the comments are also incorporated into the revised manuscript, page 3, as follows:

Moreover, all of the conjugates were structurally stable in dimethyl sulfoxide (DMSO) for at least 60 days when stored at -20°C (Supplementary Fig. 6).

In subsequent experiments, we used the nanoassemblies derived from the TPP-LA conjugate 2 that was thermodynamically stable (Supplementary Fig. 8) and was superior in terms of cytotoxic potency.
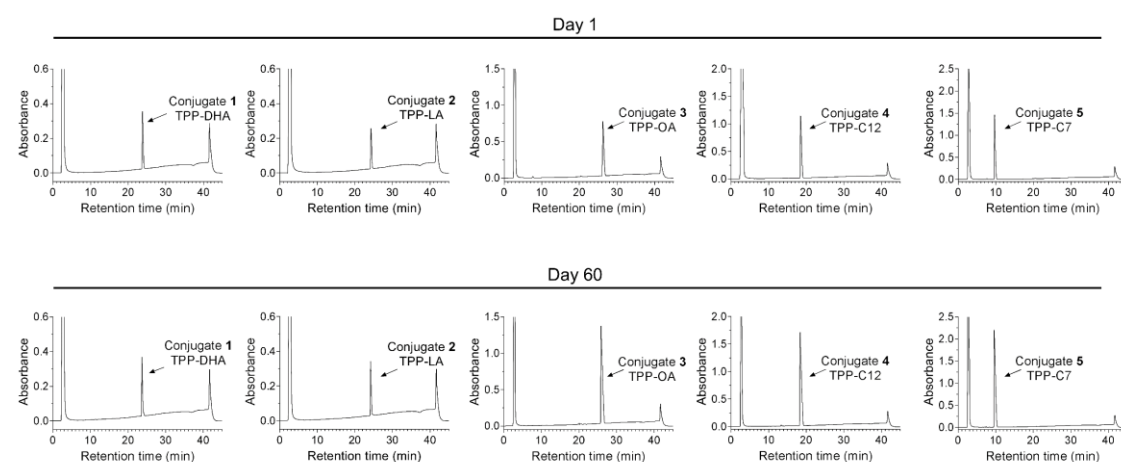
Figure S6. HPLC analysis of conjugates **1**–**5** on day 1 and day 60.
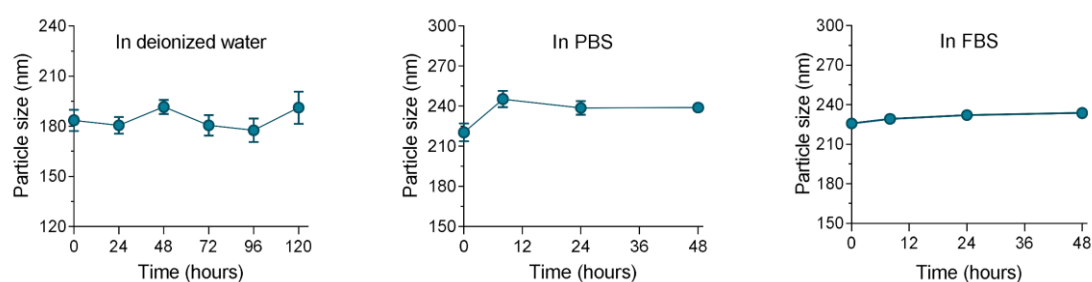
Figure S8. Stability of mtDSN-2 in deionized water, PBS and PBS containing 10% FBS tested using DLS analysis. All data are presented as the mean ± s.d. The results were shown from three biologically independent repeats.

2. In Figure 1c, it is shown that the Cy5.5-labeled nanoassemblies can co-localize with mitochondrial dyes, indicating that mtDSN-2 binds to mitochondria in the form of

nanoparticles rather than as free molecules. Please explain why TPP-LA conjugate 2 can still achieve mitochondrial targeting after forming nanoparticles.

Response:

The transmembrane potential of mitochondria is negative internally. This internal charge attracts cationic agents (e.g., lipocationic agent, mitochondrial targeting amino acid sequence) and enables enhanced electrophoretic transmembrane migration and up to 500-fold accumulation of such agents in mitochondria [7-9]. Triphenylphosphine (TPP) is a kind of delocalized lipophilic cations with the ability to transport across mitochondrial membranes. TPP consists of three phenyl groups, which results in highly lipophilic property and delocalization of positive charges on phosphonium into three aromatic rings. This facilitates the passage of TPP across the lipid membranes [10-12]. In this study, we found that the TPP-LA conjugate could recapitulate aqueous self-assembly behavior and formed spherical nanostructures, as observed by transmission electron microscopy. Dynamic light scattering revealed that the surface zeta potential of the obtained nanoassemblies (mtDSN-2) was positive (23.3 ± 6.5 mV), attributing to the positive charge in the TPP moiety, which might account for mitochondria-targeting properties of mtDSN-2.

3. By what pathway do the nanoparticles enter the cells? Do the mtDSN-2 undergo lysosome escape? Please investigate the co-localization of mtDSN-2 with lysosomes and describe the intracellular transport process of mtDSN-2.

Response:

Thank you very much for these good points. According to the Reviewer's suggestion, we investigated how mtDSN-2 were internalized by cancer cells and the subsequent intracellular fate. Using a LA-conjugated fluorescent dye Cy5.5 to label the nanoassemblies, we found that mtDSN-2 entered cells *via* an energy-dependent endocytosis pathway because lowing the temperature impeded the cellular uptake (Supplementary Fig. 9c). We next performed the cellular uptake study by pre-incubating the cells with various endocytic inhibitors, followed by flow cytometry analysis. The results revealed that cellular uptake of mtDSN-2 decreased remarkably when pre-blocking cells with cytochalasin D and chlorpromazine, suggesting the macropinocytosis and clathrin-dependent endocytosis of mtDSN-2 (Supplementary Fig. 9d). In addition, CLSM observation showed that mtDSN-2 colocalized with LysoTracker after internalization, indicating its transportation to endo/lysosomal

compartments (Supplementary Fig. 9e). After 6 h, they escaped from endo/lysosomes, presenting a staggered red signal with green LysoTracker fluorescence. To confirm whether the nanoassemblies were able to transport to the mitochondria after lysosomal escape, cells were stained with MitoTracker Green and visualized using CLSM. The results showed that the labeled nanoassemblies overlapped well with MitoTracker Green in mitochondria, with a high Pearson's colocalization coefficient (Fig. 1c and d). Isolated mitochondria from cells by flow cytometry analysis also indicated mitochondrial accumulation of mtDSN-2 (Fig. 1e). We have thoroughly revised the part of intracellular trafficking of mtDSN-2 in the revised manuscript, pages 3 and 4, as follows:

Trafficking of nanoassemblies to mitochondria causes lethal mitochondrial dysfunction

Intrigued by the strong cytotoxicity, we first endeavored to explore intracellular fate of these nanoassemblies. For this purpose, we labeled conjugate 2-assembled nanoparticles with a linoleic acid-tethered fluorescent dye, Cy5.5 (Supplementary Fig. 9a and b). We observed that the cellular uptake of these nanoparticles is energy-dependent, as lowing the temperature impeded their internalization (Supplementary Fig. 9c). Detailed inhibitor co-incubation assays revealed that the nanoassemblies predominantly entered cells through macropinocytosis and clathrin-dependent endocytosis; blocking these pathways with specific inhibitors significantly reduced their internalization (Supplementary Fig. 9d). Confocal laser scanning microscopy (CLSM) demonstrated that the nanoassemblies initially localized within endo/lysosomal compartments before escaping (Supplementary Fig. 9e). Owing to the conjugation of the TPP motif, we wondered whether the nanoassemblies could specifically target intracellular mitochondria. CLSM observation showed that the labeled nanoassemblies overlapped well with MitoTracker Green in mitochondria (with a high Pearson's colocalization coefficient of 0.6, Fig. 1c and d) rather than endoplasmic reticulum (ER) (Supplementary Fig. 9f), suggesting that the nanoassemblies indeed self-localized to mitochondria in cells. Hence, we named these mitochondria-targetable dynamic supramolecular nanoassemblies as mtDSN. By contrast, nanoassemblies lacking the TPP ligand lost the organelle specificity and were distributed throughout the cytoplasm (Fig. 1c). We then isolated mitochondria from cells and performed flow cytometry analysis to examine the mitochondrial accumulation of mtDSN-2 (Fig. 1e). In accordance with the CLSM results, mtDSN-2 displayed substantially more localization in mitochondria than the nontargetable nanoassemblies.
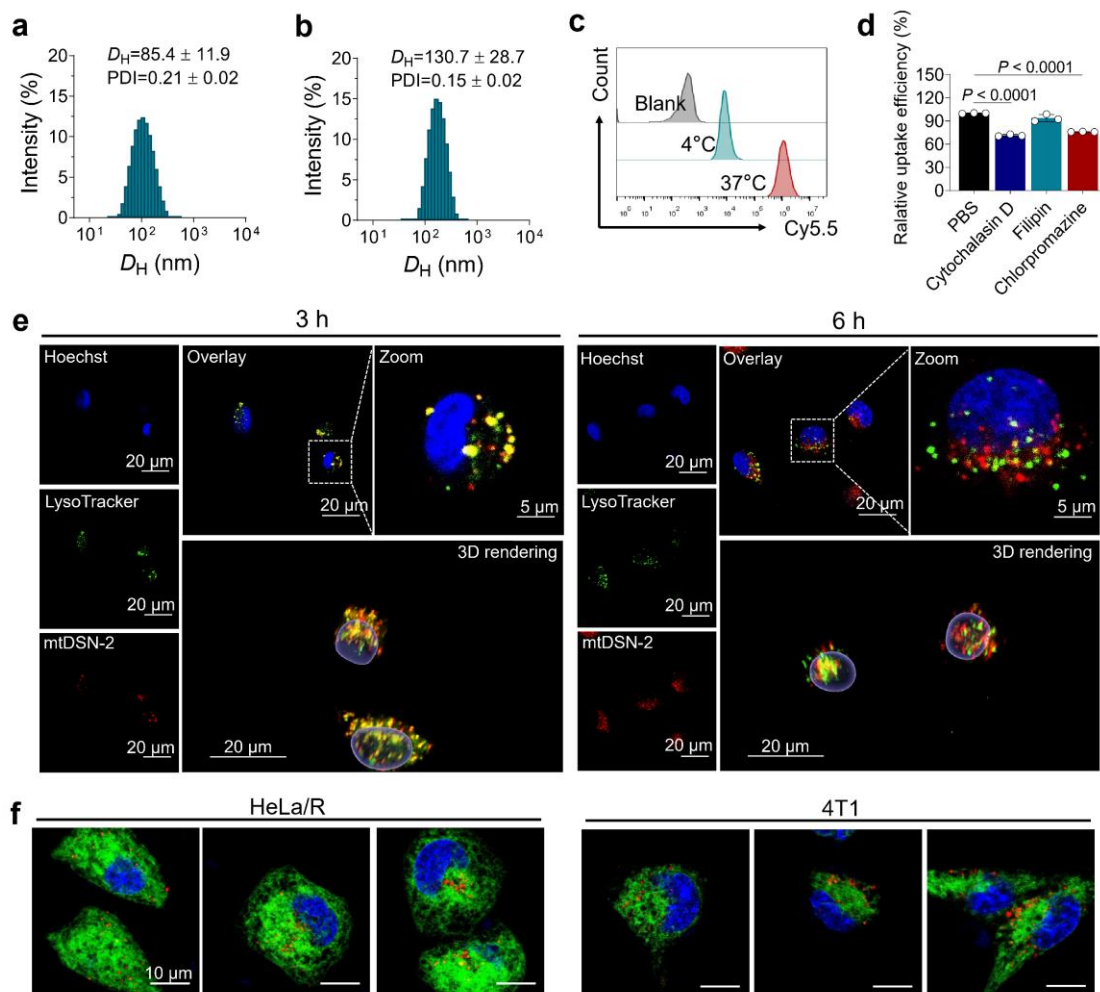
Figure S9. a, Size distribution of nanoparticles self-assembled by Cy5.5-LA. **b**, Size distribution of Cy5.5-labeled mtDSN-2. **c**, Flow cytometry analysis of the cellular uptake of mtDSN-2 at 37 and 4°C. **d**, Examination of cellular uptake of mtDSN-2 upon pretreatment with inhibitors of specific endocytosis pathways. cytochalasin D (40 μM), filipin (5 μg/mL), and chlorpromazine (10 μg/mL) were used to block macropinocytosis, caveolin-mediated endocytosis, and clathrin-mediated endocytosis, respectively. **e**, Confocal microscopy images showing the colocalization of mtDSN-2 with lysosomes. Lysosome: LysoTracker Red DND-99 (green), mtDSN-2: Cy5.5 label (red), nuclei: Hoechst 33342 (blue). **f**, Confocal microscopy images showing the colocalization of mtDSN-2 with ER. ER: ER Tracker Green (green); mtDSN-2: Cy5.5 label (red), nuclei: Hoechst 33342 (blue). The data are presented as the mean ± s.d. The results were shown from three biologically independent repeats. Statistical analysis by one-way ANOVA with Turkey's multiple comparisons test (d). Source data are provided as a Source data file.

4. Since the mitochondrial damage caused by the formulation is not selective, it can be also expected to impart the cytotoxicity onto immune cells. Thus, the authors should provide reasonable explanation why mtDSN-2 can inflame the tumors to prime the antitumor immunity.

Response:

Thanks for pointing out the important point. In this work, we demonstrated that mtDSN-2 could dynamically rewire mitochondria, induce endoplasmic reticulum stress, and cause immunogenic cell death of tumor cells by promoting CRT exposure, HMGB1 release, and ATP secretion. These danger-associated molecular patterns (DAMPs), that is, CRT, ATP, and HMGB1 bind to CD91, P2RX7, and TLR4, respectively. These events subsequently facilitate the recruitment of DCs into the tumors (stimulated by ATP), the engulfment of tumor antigens by DCs (stimulated by CRT), and optimal antigen presentation to T cells (stimulated by HMGB1). Eventually, these processes result in IL-1β- and IL-17-dependent, IFN-γ-mediated immune responses involving both γδ T cells and CTLs, and eradicate chemotherapy-resistant tumor cells [4, 13].

Although some immune cells that locally reside in the tumor microenvironment might also be partially killed, the tumor cells undergoing ICD induced by mtDSN-2 could release various DAMPs, which could function as either adjuvant or danger signals for the immune system to recruit various inflammatory and immune cells into the tumor microenvironment for robust adaptive immune response.

5. Please provide a detailed description of the experimental protocol for quantifying drug concentrations after formulation dialysis.

Response:

We have added detailed description of the experimental protocol for quantifying drug concentrations after formulation dialysis in the revised manuscript, page 13, as follows:

Preparation of dynamic supramolecular nanoassemblies

Fatty acid-TPP conjugates were dissolved in DMSO and then slowly injected into deionized water under ultrasonication to prepare the self-assembled nanoparticles. The volume ratio of DMSO to deionized water was fixed at 5%. Prior to further use, the as-prepared nano-assemblies were dialyzed against deionized water to remove the organic solvent. The drug concentration was detected via HPLC analysis at a

wavelength of 220 nm using a C8 reverse-phase column (5 µm, 250 mm × 4.6 mm, YMC Co., Ltd., Kyoto, Japan). A gradient of 50-100% acetonitrile in water within 25 min was adopted as the mobile phase at a flow rate of 1 mL/min.

Reviewer #4 (Remarks to the Author)

The manuscript "Mitochondrial Rewiring with Small-Molecule Drug-Free Nanoassemblies Unleashes Anticancer Immunity" offers a promising nondrug immune enhancer and describes its mechanisms of mitochondrial/ER-associated immunogenic cell death to overcome immunosuppression in solid tumors. Showing various in vivo evidence, the authors suggest that this new mitochondria-targeting and rewiring platform as a promising new strategy to achieve non-cytotoxic cancer therapy. I think that authors' suggestion is supported by appropriate evidence, and believe if this research further develops, it could be a promising strategy to overcome the current issues of resistance in immunotherapy. Overall, this manuscript deals with a relevant topic likely to be of considerable interest to the broader scientific cancer community, but there are some issues needed to describe more.

Response:

We thank the reviewer very much for his/her positive comments and useful suggestions, which helped us to improve the manuscript.

1. Based on my understanding, the cell death mechanisms induced by mtDSN-2 are paraptosis and apoptosis, with TPP acting as a carrier that transports LA to the mitochondria. Therefore, it seems that cell death is caused by the excessive accumulation of LA within the mitochondria. In this case, would the phenomenon observed with mtDSN-2 be the same result when treating cells with a high concentration (IC50) of LA only?

Response:

Thank you for this valuable comment. In response to the reviewer's suggestion, we explored whether a high concentration (IC_{50}) of linoleic acid (LA) could induce the same modes of cell death—paraptosis and apoptosis—as observed with mtDSN-2. The IC_{50} values for LA were determined to be 241.6 µM for HeLa/R cells and 230.6 µM

for 4T1 cells (Figure R3a). In contrast, the IC_{50} of mtDSN-2 in these cell lines was approximately 5 µM. Notably, HeLa/R and 4T1 cells displayed markedly different morphological changes at 250 µM LA compared to 5 µM mtDSN-2 treatment (Figure R3b). Specifically, the cytoplasmic vacuolation typically induced by mtDSN-2 was absent in LA-treated cells, suggesting a distinct cell death pathway mediated by high concentrations of LA. It has been previously reported that an overload of polyunsaturated fatty acids (PUFAs) may induce ferroptosis [14]. Consequently, we tested if the cytotoxic effects of high LA concentrations were due to ferroptosis. Pre-treatment of tumor cells with the ferroptosis inhibitor, ferrostatin-1, significantly improved cell viability (Figure R3c), indicating a ferroptosis-mediated death mechanism.
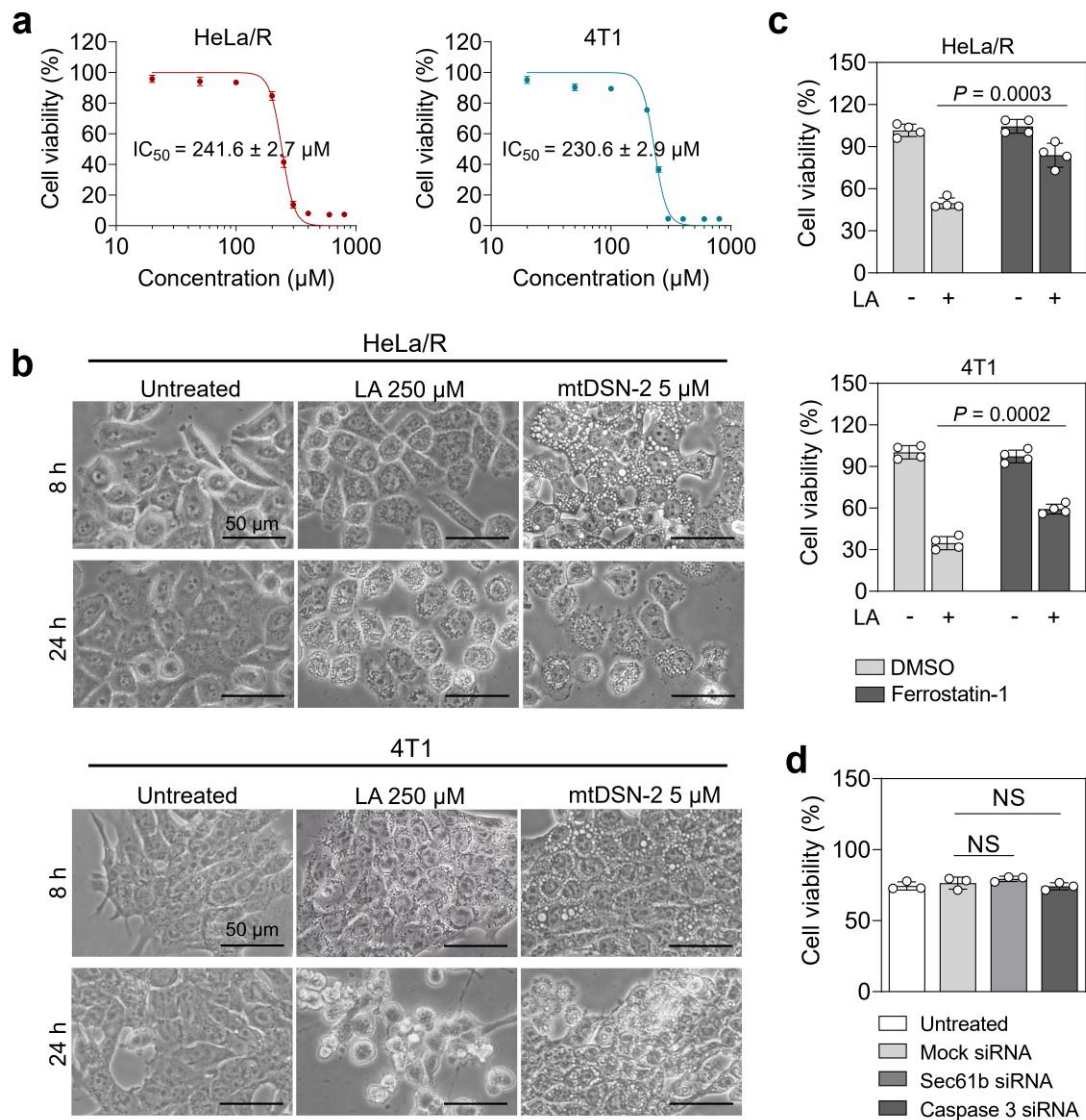

Figure R3. a, Cytotoxicity of LA in HeLa/R and 4T1 cells (48 h) determined using MTT assay (n = 4). b, Cell morphology after exposure to LA or mtDSN-2 for 8 h and 24 h.

The similar results were obtained from three biologically independent repeats. **c**, Cell viability of Hela/R and 4T1 cells pretreated with 10 μM ferroptosis inhibitor Ferrostatin-1 prior to LA exposure (n = 4). **d**, Cell viability of 4T1 cells transfected with mock, Sec61b or Caspase 3 siRNA followed by exposure to LA (n = 3). The data are presented as the mean ± s.d. Statistical analysis by Student's t test (**c**) or one-way ANOVA with Turkey's multiple comparisons test (**d**).

Moreover, we further identified the programs driving cell death using apoptosis or paraptosis-specific knockdown tumor cells. Caspase 3 and Sec61b have emerged as key contributors in mediating apoptosis and paraptosis, respectively [1-3]. We successfully constructed caspase 3 or Sec61b-knockdown 4T1 cells using siRNA mediated silencing, as indicated by the qPCR and WB verification (Supplementary Fig. 13 and Fig. 2j). Importantly, both caspase 3 and Sec61b silencing prevented the mtDSN-2-induced cell death (Fig. 2k), supporting a paraptosis/apoptosis mechanism. In contrast, both caspase 3 and Sec61b silencing failed to prevent the LA-induced cell death, suggesting that LA did not exert cytotoxicity by triggering paraptosis and apoptosis as mtDSN-2 did (Figure R3d).
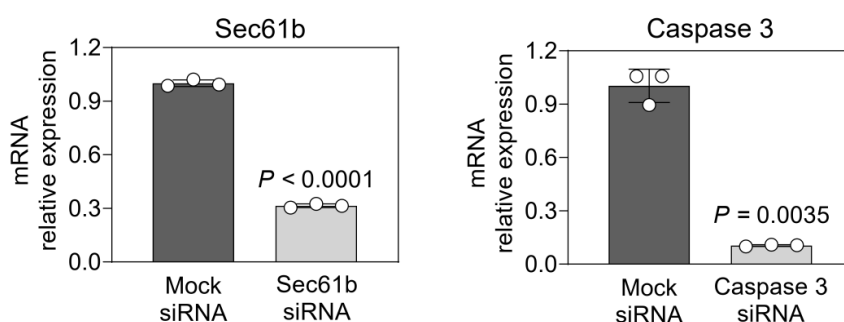
Figure S13. a, Relative mRNA expression in 4T1 cells transfected with mock (untargeted), Sec61b or caspase 3 siRNA. The data are presented as the mean ± s.d. The results were shown from three biologically independent repeats. Statistical analysis by Student's t test.
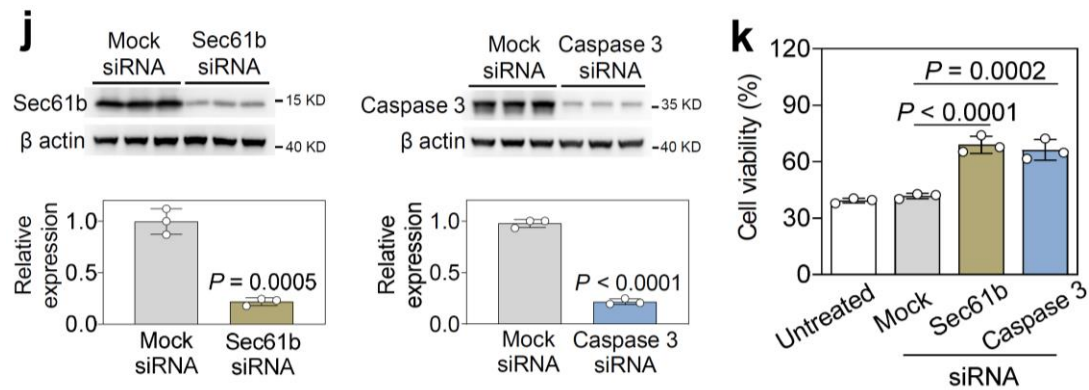
Figure 2. mtDSN induces cell death in an apoptosis and paraptosis-dependent manner. j, Immunoblotting analysis and quantification of 4T1 cells transfected with mock (untargeted), Sec61b or caspase 3 siRNA. **k**, Cell viability of 4T1 cells transfected with mock, Sec61b or caspase 3 siRNA followed by exposure to mtDSN-2.

We can therefore conclude that while LA at high concentration is cytotoxic (Figure R3a), the absence of cytoplasmic vacuolation in LA-treated cells, unlike those exposed to mtDSN-2 (Figure R3b), and the reversal of cytotoxic effects by blocking ferroptosis (Figure R3c and d), suggest distinct cell death pathways for LA and mtDSN-2. This implies that the cytotoxic mechanism of mtDSN-2 is not solely due to the selective accumulation of LA in mitochondria.

2. To verify the cytotoxicity of mtDSNs, various cell lines were used, including cisplatin-resistant cancer cells. It would be beneficial to explain the reason why you used especially cisplatin-resistant cancer cells as well.

Response:

Thank you for this good suggestion. Indeed, the primary aim of our study was to employ TPP-lipid conjugates for the targeted delivery of lipid-tethered cisplatin prodrugs to mitochondria, anticipating this approach would circumvent cisplatin resistance. Accordingly, we included various cisplatin-resistant cancer cell lines in our efficacy tests. Unexpectedly, we discovered that the TPP-lipid conjugates themselves exhibited significant cytotoxicity, effective even against cisplatin-resistant cancer cells. Further investigation revealed that the antitumor activity was strongly associated with the self-assembly behavior of these conjugates, with the assembled nanoparticles

specifically targeting mitochondria and inducing mitochondrial dysfunction. These exciting findings have spurred us to complete this project successfully.

3. To conclusively show there is a cytosolic release of cytochrome c in Figure 2k, the mitochondria should also be displayed.

Response:

Following the Reviewer's suggestion, we marked the mitochondria with TOM20, a protein localized in the outer mitochondrial membrane. TOM20 is one of the components of the TOM complex responsible for mitochondrial protein import, which is widely used as the mitochondrial marker [15]. Immunofluorescence analysis indicated that mtDSN-2 treatment readily induced cytochrome c release from mitochondria into the cytoplasm and nuclear region, which is consistent with our previous conclusion. We have updated these new results in **Fig. 2i**, and the relevant comments are included in the revised manuscript, page 5.
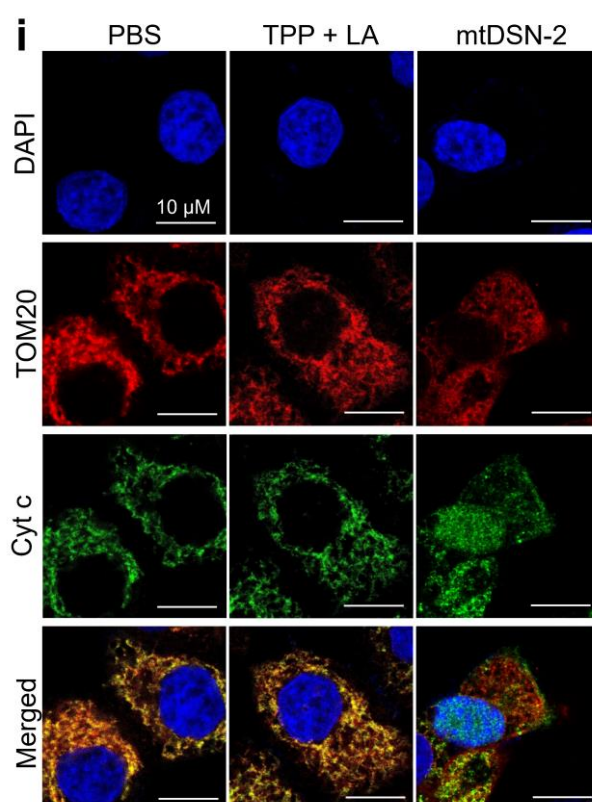

Figure 2. i, Immunofluorescence analysis of mtDSN-2-triggered release of cytochrome c (Cyt c) from mitochondria into the cytosol and nuclear region. Mitochondria: TOM20 (red), Cyt c: antibody against Cyt c (green), nuclei: DAPI (blue). Similar results were obtained from three biologically independent repeats.

4. Beside to HRI-dependent eIF2a phosphorylation (line 253), there is PERK activation by mtDSN-2 (Fig. 3o). Furthermore, ER swelling is evident in Figure 3n. Based on that I am curious whether there is a direct impact or accumulation of mtDSN-2 on the ER. Additionally, is there any swelling of the ER observed in TEM consistent with fluorescent image in Figure 3n?

Response:

Many thanks for these points. To figure out whether there is a direct impact or accumulation of mtDSN-2 on the ER, we investigated the colocalization of mtDSN-2 with ER (Supplementary Fig. 9f). Unlike the highly overlapped signals of mtDSN-2 with that of MitoTracker Green in cells, the signal distribution of mtDSN-2 is staggered with that of ER Tracker Green, suggesting that mtDSN-2 specifically target intracellular mitochondria rather than ER. The relevant comments are supplemented in the revised manuscript, page 4, as follows:

CLSM observation showed that the labeled nanoassemblies overlapped well with MitoTracker Green in mitochondria (with a high Pearson's colocalization coefficient of 0.6, Fig. 1c and d) rather than endoplasmic reticulum (ER) (Supplementary Fig. 9f), suggesting that the nanoassemblies indeed self-localized to mitochondria in cells.
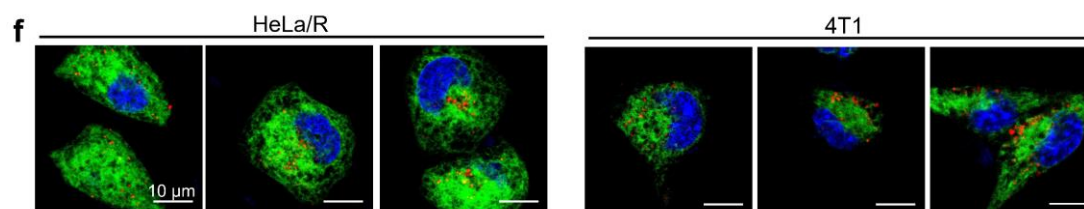

Figure S9. f, Confocal microscopy images showing the colocalization of mtDSN-2 with ER. ER: ER Tracker Green (green); mtDSN-2: Cy5.5 label (red), nuclei: Hoechst 33342 (blue). The results were shown from three biologically independent repeats.

In addition, we observed the swelling of the ER using TEM analysis in both HeLa/R (Fig. 1f) and 4T1 cells (supplementary Fig. 10), which is consistent with the results of fluorescent images in Fig. 3n. We used green arrows and red asterisks to indicate the damaged mitochondria and swelling endoplasmic reticulum, respectively. The relevant comments are also supplemented in the revised manuscript, page 4, as follows:

Mitochondrial damages similar to that observed in HeLa/R cells were also evident

in mtDSN-2-treated 4T1 cells (Supplementary Fig. 10).
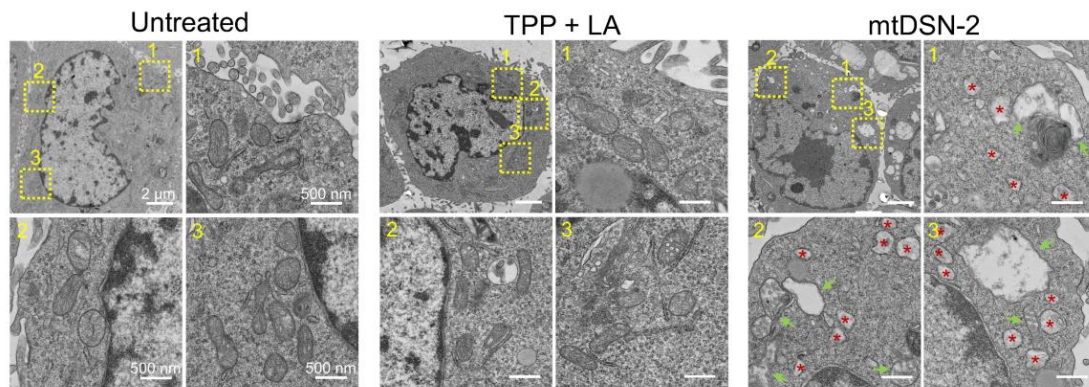
Figure S10. TEM images of mitochondrial ultrastructure in 4T1 cancer cells following various treatments. Green arrows point to damaged mitochondria, while red asterisks mark areas of swelling endoplasmic reticulum. These images represent findings from three biologically independent experiments.

5. In Figure 3e, measuring the extracellular level of HMGB1 rather than its cytosolic level would provide more accurate evidence of immunogenic cell death (ICD).

Response:

According to the Reviewer's suggestion, we additionally measured the extracellular level of HMGB1 using ELISA kits. Significant HMGB1 release to the cell culture media was observed in both HeLa/R and 4T1 cells after mtDSN-2 treatment. The new data are presented in Fig. 3e, and the comments are also supplemented in the revised manuscript, page 5, as follows:

mtDSN-2 caused a significant HMGB1 release from the nucleus to the cytoplasm and extracellular medium in both tested cancer cell lines (Fig. 3d and e).
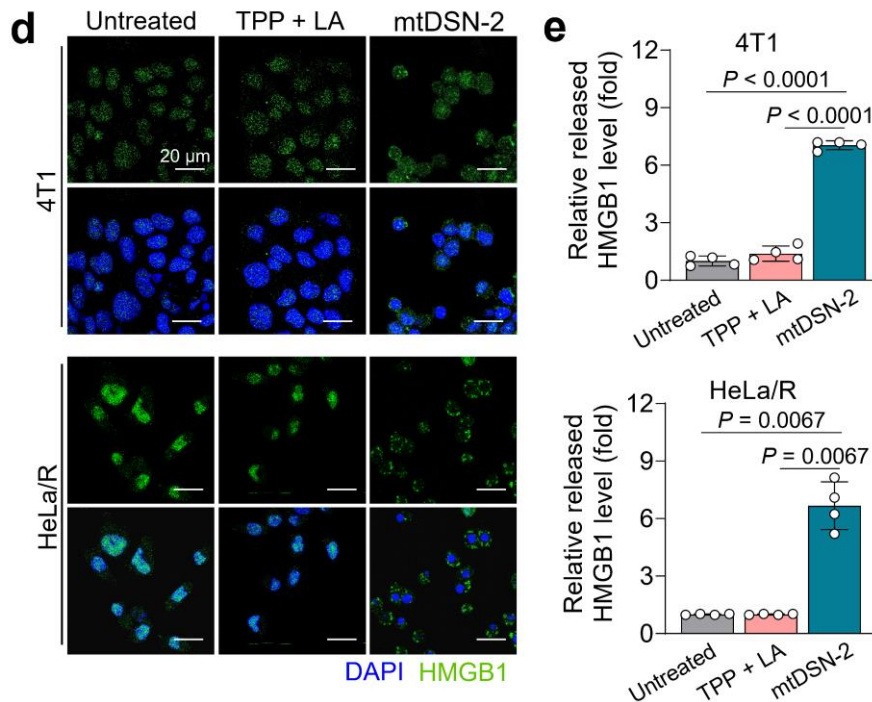
Figure 3. d, Confocal microscopy images showed HMGB1 release from the nuclei to the cytoplasm after mtDSN-2 treatment. HMGB1: antibody against HMGB1 (green), nuclei: DAPI (blue). **e**, Extracellular HMGB1 release determined by ELISA. The representative images of panels (**d**) were repeated in two biologically independent cell lines. n = 4 biologically independent repeats (**e**). Statistical analysis by one-way ANOVA with Turkey's multiple comparisons test.

6. The evidence for paraptosis appears insufficient, as it relies solely on ER/mitochondria swelling and death blocked by CHX. Since CHX is known to inhibit not only paraptosis but also ER stress-induced cell death, it appears crucial to present changes in other markers of paraptosis.

Response:

Thanks for these important comments. Paraptosis is a programmed cell death characterized by cytoplasmic vacuolation and mitochondrial and/or ER swelling [16]. However, detailed molecular mechanism of paraptosis remains unclarified. Previous studies showed that paraptosis was associated with the redox and ion (e.g., Ca^{2+}) homeostasis alteration, or the accumulation of misfolded proteins in the ER, leading to proteostasis disruption and excessive ER stress responses [17, 18]. Moreover, paraptosis requires de novo protein synthesis, which can be successfully blocked by the translation inhibitor cycloheximide (CHX) [1]. In this study, we have demonstrated that

mtDSN-2 exposure could lead to unregulated reactive oxygen species (ROS) production (Fig. 3j, k and Supplementary Fig. 16), extensive cytoplasmic vacuolation associated with mitochondrial and ER swelling (Fig. 1f, 2e, 3n, and Supplementary Fig. 10, 11).

As the Reviewer notes, the evidence for paraptosis appears insufficient. We here additionally examined ubiquitination of cellular proteins using immunoblotting, which indicates the perturbation of proteostasis (New data in Supplementary Fig. 17). The data are discussed in the revised manuscript, page 6, as follows:

Subsequently, the loss of ER proteostasis was also observed, evidenced by an increase in ubiquitinated proteins in mtDSN-2-treated cells (Supplementary Fig. 17)
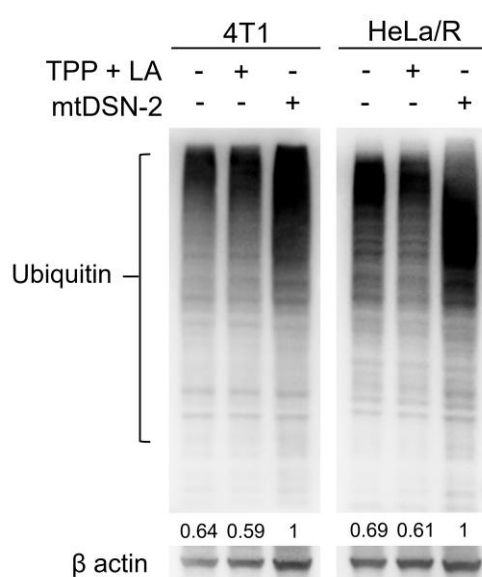
Figure S17. Western blot analysis of ubiquitinated proteins after treatment (5 µM for 36 h). Band intensities were quantified from the 8-bit digital image by densitometry in ImageJ and are shown normalized to the mtDSN-2 lane. The similar results were repeated in two biologically independent experiments.

We also assessed several ER stress marker proteins (e.g., phosphor-eIF2α, ATF4, and CHOP). The results showed that mtDSN-2 induced increased levels of these critical biomarkers, suggesting the excessive ER stress responses (Fig. 3o and p).
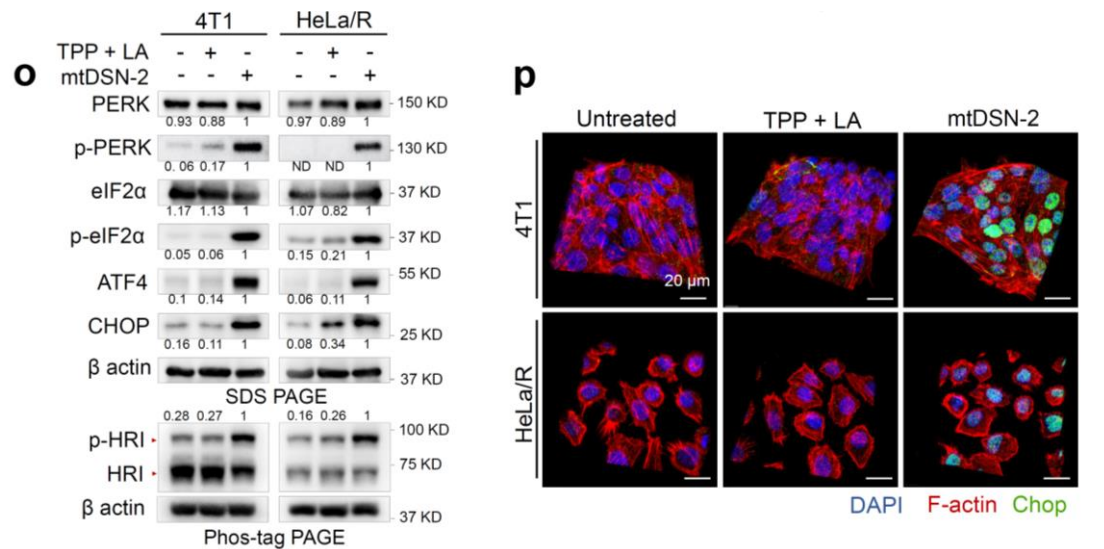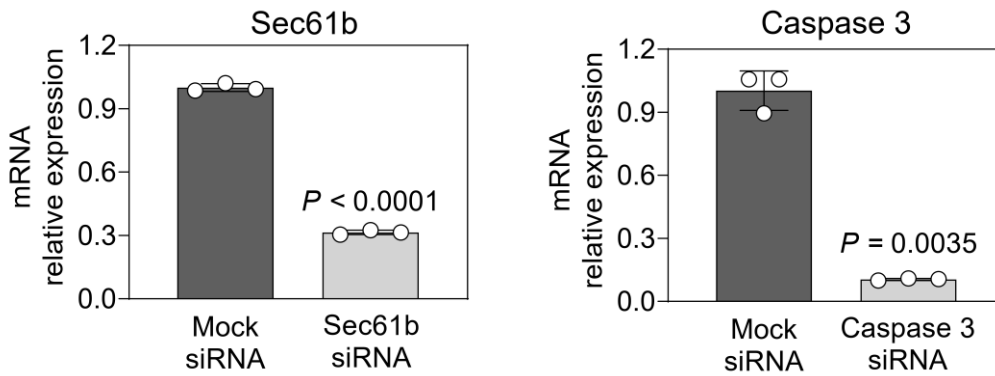
Figure 3. o, Western blot analysis of ER-stress related protein in cells treated with mtDSN-2 (5 µM for 36 h). Cell lysates were subjected to immunoblotting for the indicated proteins and their phosphorylation. In the phos-tag PAGE assay, a phos-tag gel was used to resolve the protein phosphorylation, which can be assessed by the mobility shift. Band intensities were quantified from the 8-bit digital images by densitometry in ImageJ and are shown normalized to the mtDSN-2 lane for each target. ND, not detected. **p**, Confocal microscopy images showing CHOP expression in tumor cells after different treatments. CHOP: antibody against CHOP (green), F-actin: Rhodamine Phalloidin (red), nuclei: DAPI (blue). The representative images of panels (**p**) were repeated in two biologically independent cell lines. The similar results were repeated in two biologically independent experiments (**o**).
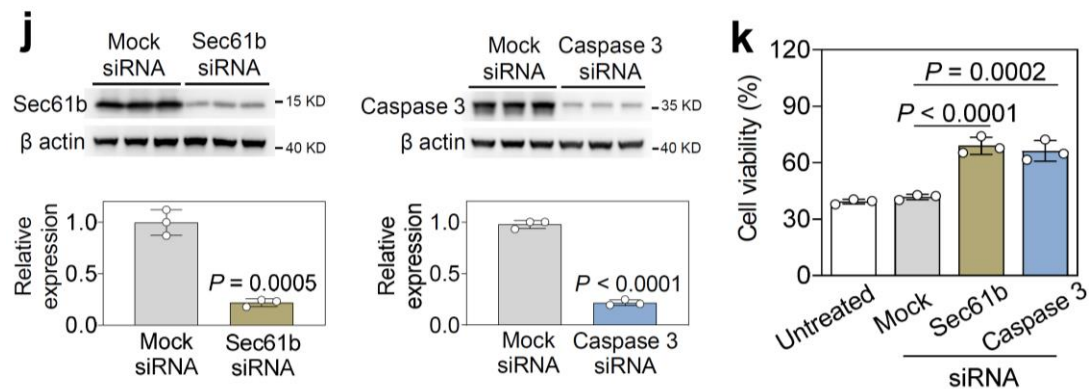
Moreover, treatment with *de novo* translation inhibitor CHX effectively blocked mtDSN-induced cell death and prevented paraptosis vacuolation morphology (Fig. 2d and f).

Sec61b has emerged as a key contributor in mediating paraptosis. Sec61b silencing was reported to inhibit paraptosis. We therefore additionally constructed sec61b-knockdown 4T1 cells using siRNA-mediated silencing, as indicated by the qPCR and western blot results (Supplementary Fig. 13 and Fig. 2j). Sec61b knockdown inhibited mtDSN-2-triggered cell death (Fig. 2k), supporting the paraptosis-associated mechanism. The relevant results are presented in Fig. 2j, k and Supplementary Fig. 13, and the results are commented in the revised manuscript, page 5, as follows:

Sec61b and caspase 3 are crucial in mediating paraptosis and apoptosis, respectively. Intriguingly, we found that silencing Sec61b and caspase 3 inhibited the mtDSN-2-induced cell death (Fig. 2j, k and Supplementary Fig. 13). This finding further supports the proposed mechanism by which mtDSN-2 induces lethal mitochondrial paraptosis/apoptosis.

Figure S13. a, Relative mRNA expression in 4T1 cells transfected with mock (untargeted), Sec61b or caspase 3 siRNA. The data are presented as the mean ± s.d. The results were shown from three biologically independent repeats. Statistical analysis by Student's t test.

Figure 2. mtDSN induces cell death in an apoptosis and paraptosis-dependent manner. j, Immunoblotting analysis and quantification of 4T1 cells transfected with mock (untargeted), Sec61b or caspase 3 siRNA. **k**, Cell viability of 4T1 cells transfected with mock, Sec61b or caspase 3 siRNA followed by exposure to mtDSN-2.
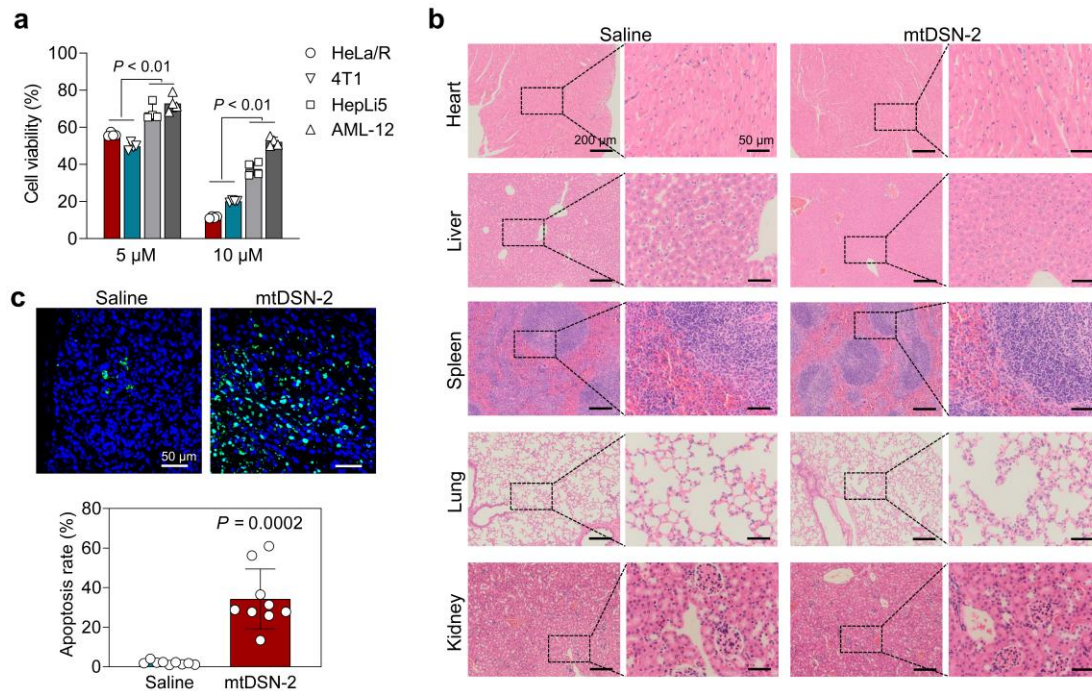
7. Have you conducted tests on the impact of mtDSN-2 on normal cells? Does the accumulation of mtDSN-2 on the mitochondria of normal cells or immune cells occur? What is the cancer-specific targeting mechanism of mtDSN-2?

Response:

Given that the selective accumulation of mtDSN-2 in mitochondria mainly attributes to the presence of the mitochondria-targeting moiety TPP, mtDSN-2 could also be internalized by normal cells and causes mitochondrial dysfunction, thereby yielding impacts on normal cells. To address the Reviewer's question here, we compared the cytotoxicity of mtDSN-2 on normal cells and tumor cells using MTT assay. 48 h-incubation of mtDSN-2 produced lower cytotoxicity on normal hepatocytes (e.g., HepLi5 and AML12) than on tumor cells (HeLa/R and 4T1) ($P < 0.01$, supplementary Fig. 30a).

In addition, mtDSN-2 was intratumorally administrated for all *in vivo* studies in this work. In combination with our response to Reviewer 1, point #2, we have additionally established the orthotopic 4T1 tumor model to evaluate the safety profile of mtDSN-2 by intratumoral administration. After two injections of mtDSN-2, the tumors and major organs were collected and subjected to immunohistochemical analysis. As shown in Supplementary Fig. 30c, mtDSN-2 induced extensive intratumoral apoptosis indicated by TUNEL staining. However, the major organs (i.e., heart, liver, spleen, lung and kidney) of mice did not show obvious damage after mtDSN-2 treatment (Supplementary Fig. 30b), which were comparable with that of mice receiving saline by H&E analysis. The relevant results are presented in Supplementary Fig. 30, and the comments are also supplemented in the revised manuscript, page 11, as follows:

Indeed, mtDSN-2 was less cytotoxic on hepatocytes than on cancer cells observed in in vitro assays (Supplementary Fig. 30a). Intratumoral administration of mtDSN-2 did not impart any side effects on major healthy tissues (Supplementary Fig. 30b) while inducing extensive apoptotic cell death in tumors (Supplementary Fig. 30c), suggesting its favorable safety profile for the preclinical use.

Figure S30. a, Cytotoxicity of mtDSN-2 (5 μM or 10 μM for 48 h) in cancer cells (HeLa/R) and hepatocytes (AML12 and HepLi5) determined using MTT assay (n = 4). **b**, H&E staining of the major organs (n = 3 mice/group) after drug administration. **c**, Immunohistochemical analysis of the tumor apoptosis by TUNEL staining (n = 3 mice/group). The data are presented as the mean ± s.d. Statistical analysis by one-way ANOVA with Turkey's multiple comparisons test, Brown-Forsythe and Welch ANOVA with Dunnett's T3 multiple comparisons test (**a**) and Student's t test (**c**).

8. A more detailed discussion is needed on the underlying mechanism (or possible explanation) by which mitochondrial stress induction by mtDNS-2 lead to ICD.

Response:

Thanks for this comment. Reactive oxygen species (ROS) production and ER stress are essential prerequisites for ICD induction [4]. Using the ROS probes such as MitoSOX and 2',7'-dichlorofluorescein diacetate (DCFH-DA), we confirmed that mtDSN-2 significantly increased mitochondrial superoxide levels and cellular ROS levels in cancer cells (Fig. 3j, k and Supplementary Fig. 16). As ER and mitochondria are tightly juxtaposed in structure and associated in function, we speculated that excessive mitochondria perturbation and overloading of ROS might lead to ER dysfunction and stress. We indeed observed the significant ER mass enlargement and swelling (Fig. 3l-n), the loss of cellular proteostasis (Supplementary Fig. 17), and increased levels of ER stress marker proteins in tumor cells exposed to mtDSN-2 (Fig.

3o), suggesting the proposed ER stress. In respect of the Reviewer's suggestion, we here added the discussion on the underlying mechanism of ICD induced by mtDNS-2-mediated mitochondrial stress in the revised manuscript, page 11, as follows:

Mechanistic experiments revealed that the mtDSN platform substantially impeded mitochondrial biogenesis in tumor cells. The overwhelming mitochondrial stress, induced by mtDSN-2, also perturbed ER homeostasis through excessive ROS production and potential imbalance in substance exchanges, leading to irreversible ER stress. This pronounced ER stress facilitated the activation of subsequent cellular death programs through both paraptosis and apoptosis pathways. Additionally, we observed that stressed and injured tumor cells emitted various DAMPs, including surface-exposed CRT, passively released HMGB1, and secreted ATP. These danger signals stimulated immunological responses by eliciting the ICD cascade and converted immunologically silent tumors into inflamed ones.

9. Please write the concentrations of each inhibitor presented in Figure 2.

Response:

Thank you for your careful reading. We have added the concentrations of each inhibitor in the Fig. 2 legend in the revised manuscript, page 25, as follows:

Figure 2. c and **d**, Cell viability of Hela/R and 4T1 cells pretreated with ferroptosis inhibitor Ferrostatin-1 (10 μM), necroptosis inhibitor Necrostatin-1 (10 μM), pyroptosis NLRP3 inhibitor Dapansutrile (10 μM), paraptosis inhibitor cycloheximide (CHX, 10 μM), or pan-caspase apoptosis inhibitor Z-VAD-FMK (40 μM) before incubation with or without mtDSN-2. *P* indicates the significance relative to DMSO treatment.

10. The composition of each mtDSN conjugate 1 to 5 should be specified in the text. For example, specify that conjugate 2 is TPP-LA in lines 92-93.

Response:

We have specified the conjugates in the revised manuscript, page 3, according to your comments.

References

1. Mandula, J.K. *et al.* Ablation of the endoplasmic reticulum stress kinase PERK induces paraptosis and type I interferon to promote anti-tumor T cell responses. *Cancer Cell* **40**, 1145-1160 (2022).

2. Lang, S. *et al.* An Update on Sec61 Channel Functions, Mechanisms, and Related Diseases. *Front. Physiol.* **8**, 887 (2017).

3. Porter, A.G. & Jänicke, R.U. Emerging roles of caspase-3 in apoptosis. *Cell Death Differ.* **6**, 99-104 (1999).

4. Krysko, D.V. *et al.* Immunogenic cell death and DAMPs in cancer therapy. *Nat. Rev. Cancer* **12**, 860-875 (2012).

5. Vistica Sampino, E. *et al.* Comparative flow cytometry-based immunophenotyping analysis of peripheral blood leukocytes before and after fixation with paraformaldehyde. *J. Immunol. Methods* **511**, 113379 (2022).

6. Zhou, F. *et al.* Tumor Microenvironment-Activatable Prodrug Vesicles for Nanoenabled Cancer Chemoimmunotherapy Combining Immunogenic Cell Death Induction and CD47 Blockade. *Adv. Mater.* **31**, e1805888 (2019).

7. Frantz, M.C. & Wipf, P. Mitochondria as a target in treatment. *Environ. Mol. Mutagen.* **51**, 462-475 (2010).

8. Shin, W.S. *et al.* Mitochondria-targeted aggregation induced emission theranostics: crucial importance of in situ activation. *Chem. Sci.* **7**, 6050-6059 (2016).

9. Noh, I. *et al.* Enhanced Photodynamic Cancer Treatment by Mitochondria-Targeting and Brominated Near-Infrared Fluorophores. *Adv. Sci. (Weinh)* **5**, 1700481 (2018).

10. Murphy, M.P. Targeting lipophilic cations to mitochondria. *Bba-Bioenergetics* **1777**, 1028-1031 (2008).

11. Millard, M. *et al.* Preclinical Evaluation of Novel Triphenylphosphonium Salts with Broad-Spectrum Activity. *Plos One* **5**, e13131 (2010).

12. Yamada, Y. & Harashima, H. Mitochondrial drug delivery systems for macromolecule and their therapeutic application to mitochondrial diseases. *Adv. Drug Deliver. Rev.* **60**, 1439-1462 (2008).

13. Kroemer, G., Galluzzi, L., Kepp, O. & Zitvogel, L. Immunogenic Cell Death in Cancer Therapy. *Annu. Rev. Immunol.* **31**, 51-72 (2013).

14. Dierge, E. *et al.* Peroxidation of n-3 and n-6 polyunsaturated fatty acids in the acidic tumor environment leads to ferroptosis-mediated anticancer effects. *Cell Metab.* **33**, 1701-1715 e1705 (2021).

15. Su, J. *et al.* Structural basis of Tom20 and Tom22 cytosolic domains as the human TOM complex receptors. *Proc. Natl. Acad. Sci. U. S. A.* **119**, e2200158119 (2022).

16. Sperandio, S., de Belle, I. & Bredesen, D.E. An alternative, nonapoptotic form of programmed cell death. *Proc. Natl. Acad. Sci. U. S. A.* **97**, 14376-14381 (2000).

17. Chen, F.Q. *et al.* Targeting paraptosis in cancer: opportunities and challenges. *Cancer Gene Ther.* **31**, 349-363 (2024).

18. Hanson, S. *et al.* Paraptosis: a unique cell death mode for targeting cancer. *Front. Pharmacol.* **14**, 1159409 (2023).

REVIEWERS' COMMENTS

Reviewer #1 (Remarks to the Author):

The authors have improved their work and answered all questions posed by the four reviewers.

They added mechanistic clues and explored additional tumor models.

Many of the queries have been addressed experimentally thus underlining the robustness and reproducibility of the presented data.

Annexed raw data supports (much needed) scientific transparency.

Reviewer #2 (Remarks to the Author):

The author has already fully revised the manuscript according to the previous comments raised by the reviewers. I support the acceptance of the manuscript right now.

Reviewer #3 (Remarks to the Author):

My concerns have been well corrected in the revised manuscript. Now I suggested that it can be accepted.

Reviewer #4 (Remarks to the Author):

I am satisfied with the revision, and have no further revision request.

REVIEWERS' COMMENTS

Reviewer #1 (Remarks to the Author):

The authors have improved their work and answered all questions posed by the four reviewers.

They added mechanistic clues and explored additional tumor models.

Many of the queries have been addressed experimentally thus underlining the robustness and reproducibility of the presented data.

Annexed raw data supports (much needed) scientific transparency.

Reviewer #2 (Remarks to the Author):

The author has already fully revised the manuscript according to the previous comments raised by the reviewers. I support the acceptance of the manuscript right now.

Reviewer #3 (Remarks to the Author):

My concerns have been well corrected in the revised manuscript. Now I suggested that it can be accepted.

Reviewer #4 (Remarks to the Author):

I am satisfied with the revision, and have no further revision request.

RESPONSE TO THE REVIEWERS' COMMENTS

We would like to express our sincere appreciation to the comments from the four reviewers to help us improve the quality of our work.